

# A fully relativistic description of spin-orbit torques by means of linear response theory

S. Wimmer,<sup>\*</sup> K. Chadova, M. Seemann, D. Ködderitzsch, and H. Ebert<sup>†</sup>  
*Department Chemie/Phys. Chemie, Ludwig-Maximilians-Universität München, Germany*  
 (Dated: 14th October 2018)

Symmetry and magnitude of spin-orbit torques (SOT), i.e., current-induced torques on the magnetization of systems lacking inversion symmetry, are investigated in a fully relativistic linear response framework based on the Kubo formalism. By applying all space-time symmetry operations contained in the magnetic point group of a solid to the relevant response coefficient, the torkance expressed as torque-current correlation function, restrictions to the shape of the direct and inverse response tensors are obtained. These are shown to apply to the corresponding thermal analogues as well, namely the direct and inverse thermal SOT in response to a temperature gradient or heat current. Using an implementation of the Kubo-Bastin formula for the torkance into a first-principles multiple-scattering Green's function framework and accounting for disorder effects via the so-called coherent potential approximation (CPA), all contributions to the SOT in pure systems, dilute as well as concentrated alloys can be treated on equal footing. This way, material specific values for all torkance tensor elements in the fcc (111) trilayer alloy system Pt|Fe<sub>x</sub>Co<sub>1-x</sub>|Cu are obtained over a wide concentration range and discussed in comparison to results for electrical and spin conductivity, as well as to previous work – in particular concerning symmetry w.r.t. magnetization reversal and the nature of the various contributions.

PACS numbers: 61.50.Ah, 72.15.Qm, 75.70.Tj, 75.76.+j

## I. INTRODUCTION

Spin-orbit torques (SOT), denoting the response of a magnetization to an electric current by changing its orientation, have evolved from a theoretical conjecture<sup>1-3</sup> via experimental verification<sup>4-6</sup> to their imminent technological application in SOT-MRAM devices<sup>7</sup> in a remarkably short period of time. This can be attributed to the fact that unlike most<sup>8</sup> other ways of defined manipulation of magnetic moments it does not require external magnetic fields or auxiliary magnetic layers, offering an enormous advantage concerning information storage density, non-volatility and scalability.<sup>9</sup> The combined effect of spin-orbit interaction and exchange coupling in systems lacking inversion symmetry offers thus the possibility to switch the magnetization of spintronics devices by applying an electric current. Unlike its close relative, the spin-transfer torque mechanism,<sup>10,11</sup> it does not rely on the presence of a “polarizer” magnetic layer, allowing for much simpler device architecture and reducing necessary critical current densities.<sup>12</sup> The intrinsic relativistic spin-orbit interaction can transfer orbital to spin angular momentum in a magnetic material having a suitable structure, leading to an effective magnetic field exerting a torque on the magnetization.

Recent experiments<sup>13-15</sup> were able to measure the SOT directly as a function of magnetization direction, whereas earlier evidence has only been indirect.<sup>4-6,9,16-18</sup> Two symmetrically distinct contributions to the SOT could be observed this way, one being even and the other odd with respect to magnetization reversal. To lowest order in the magnetization direction  $\hat{\mathbf{m}}$ , the even torque in response to an in-plane current  $\mathbf{j}$  was found to go by  $\hat{\mathbf{m}} \times (\mathbf{j} \times \hat{\mathbf{m}})$  while the odd one scales with  $\hat{\mathbf{m}} \times \mathbf{j}$ . While initial work on spin-orbit torques was

focused on transition metal FM|NM bilayers<sup>5,6</sup> or dilute magnetic semiconductors,<sup>4</sup> recent experiments<sup>19-22</sup> demonstrate the possibility to switch ferromagnetic moments by SOTs originating from antiferromagnets, as predicted theoretically.<sup>23</sup> On the ferromagnetic side it could be shown that magnetic insulators can be switched by SOTs as well.<sup>24</sup> Exploiting the large spin-orbit coupling of Bismuth and the pronounced ferromagnetism of Cr-doped Bi<sub>x</sub>Sb<sub>1-x</sub>Te<sub>3</sub>, topological insulator heterostructures were shown to be promising candidates for SOT-based memory and logic devices.<sup>25,26</sup> Although the nature of the spin-orbit torque certainly is not yet fully understood in all details, its ability to deterministically switch magnetic moments, without the need for external magnetic fields,<sup>27</sup> has been demonstrated beyond doubt. Currently, experimental research is already heading towards fully functional devices,<sup>28,29</sup> en route exposing further interesting aspects of SOTs.<sup>30,31</sup>

Early theoretical work on the SOT in bilayer systems proposed two distinct mechanisms, namely a torque arising from the Rashba effect at the asymmetric interface,<sup>2,32-34</sup> and a spin transfer torque due to the spin current generated in the heavy-metal layer by the spin Hall effect.<sup>17,18,35</sup> The “Rashba”-torque was initially found to be dominated by a field-like component<sup>32,36,37</sup> being odd w.r.t. magnetization reversal, whereas the “spin Hall”-torque was believed to consist mostly of an even (anti-)damping- or spin transfer-like contribution.<sup>9,17,18,37</sup> This picture has however turned out to be too simple,<sup>13,14</sup> as these mechanisms appear to be only the limiting cases of a more complex scenario,<sup>13,38</sup> involving terms of higher-order in the magnetization direction<sup>13</sup> and in addition an intrinsic contribution, arising from the band structure in a single ferromagnetic layer alone.<sup>39,40</sup> First-principles calculations of the torkance tensor<sup>41-43</sup> can be used to

help to disentangle the various contributions by providing model-independent material parameters. The pioneering works of Freimuth *et al.*<sup>42,43</sup> demonstrated this for FM|NM bilayer systems using the Kubo linear response formalism to calculate layer-resolved torkances.

It has been noted quite early on,<sup>33–35,44</sup> that there exists of course an Onsager reciprocal to the spin-orbit torque, i.e., by interchanging perturbation (electric field or charge current) and response (torque on the magnetization) one arrives at the inverse spin-orbit torque (ISOT), describing the electric field induced by magnetization dynamics.<sup>45</sup> The reciprocity of the two, SOT and ISOT, has been discussed recently in great detail by Freimuth *et al.*,<sup>46</sup> who noted that both phenomena can be described by the torkance tensor. In this work, by performing a symmetry analysis of the linear response expressions describing SOT and ISOT, we will give explicit tensor shapes for both properties in terms of the torkance, thereby demonstrating, where applicable, the presence and exact form of their reciprocity. As will be demonstrated, these shapes remain unchanged when replacing the electric field by a temperature gradient, giving a justification for the use of a Mott-like expression for direct and inverse thermal SOT discussed by Géronton *et al.*<sup>47</sup> and Freimuth *et al.*<sup>48</sup>.

The present paper focuses on two aspects of the spin-orbit torque that have, to our knowledge, not been studied before. Firstly, an extensive symmetry analysis based on group-theoretical grounds and not restricted to special cases is performed that allows determining the tensor shapes of both direct and inverse SOT from their respective Kubo linear response expressions, based on the magnetic point group alone. Secondly, by making use of the Coherent Potential Approximation (CPA) within multiple scattering theory the possibility to study the concentration-dependence of the torkance in alloys is demonstrated, thereby opening the route for a materials design approach to the SOT.

This paper is organized as follows: In Section II we

introduce the underlying linear response formalism used to calculate the torkance tensor, discuss its implementation into a multiple scattering framework, with particular emphasis on the treatment of disorder, and finally outline the application of symmetry considerations leading to restrictions to the tensor shapes of both, direct and inverse spin-orbit torques. The outcome of this group-theoretical analysis for all magnetic point groups allowing for the existence of a finite magnetization will be presented together with corresponding results for the electrical and spin conductivity tensors. In Section III we present the results of our numerical investigations on a Pt|Fe<sub>x</sub>Co<sub>1-x</sub>|Cu trilayer system, highlighting the impact of disorder effects (impurity scattering) on the various contributions to the torkance. By comparing concentration-dependent results for the torkance tensor with such for the spin Hall conductivity we will discuss their (partial) interconnection. Finally, contact will be made to previous work, in particular concerning the separation of the torkance into contributions based on the structure of the linear response expression (Fermi sea and Fermi surface terms) and on symmetry arguments (even or odd symmetry w.r.t. magnetization reversal). We conclude with a summary of the presented and an outlook on future work in Section IV.

## II. FORMALISM

A well-known application of Kubo's linear response formalism is the derivation of an expression for the electrical conductivity tensor  $\underline{\sigma}$  that describes the electric current density  $\mathbf{j} = \underline{\sigma} \mathbf{E}$  in response to an electric field  $\mathbf{E}$ . In analogy one can derive an expression for the torkance tensor  $\underline{\mathbf{t}}$  that gives the torque  $\mathbf{T} = \underline{\mathbf{t}} \mathbf{E}$  as a response to  $\mathbf{E}$ .<sup>42,43</sup> Replacing the operator  $\hat{j}_\mu$  representing the component  $\mu$  of the current density by the operator  $\hat{T}_\mu$  for the torque one can straightforwardly adopt the derivation of the so-called Kubo-Bastin formula for  $\underline{\sigma}$ ,<sup>49,50</sup> leading to a corresponding expression for the torkance  $\underline{\mathbf{t}}$ .<sup>51</sup>

$$t_{\mu\nu} = -\frac{\hbar}{4\pi V} \int_{-\infty}^{\infty} d\varepsilon \frac{df(\varepsilon)}{d\varepsilon} \text{Tr} \left\langle \hat{T}_\mu (G^+ - G^-) \hat{j}_\nu G^- - \hat{T}_\mu G^+ \hat{j}_\nu (G^+ - G^-) \right\rangle + \frac{\hbar}{4\pi V} \int_{-\infty}^{\infty} d\varepsilon f(\varepsilon) \text{Tr} \left\langle \hat{T}_\mu G^+ \hat{j}_\nu \frac{dG^+}{d\varepsilon} - \hat{T}_\mu \frac{dG^+}{d\varepsilon} \hat{j}_\nu G^+ - \text{“} (G^+ \rightarrow G^-) \text{“} \right\rangle, \quad (1)$$

where  $V$  is the volume of the unit cell and  $f(E)$  is the Fermi distribution function. This implies that in the limit  $T \rightarrow 0$  K for the temperature the first term in Eq. (1) has to be evaluated only for the Fermi energy  $E_F$  (Fermi surface term  $t_{\mu\nu}^I$ ), while the second one requires an integration over the occupied part of the valence band (Fermi sea term  $t_{\mu\nu}^{II}$ ).

The operator  $\hat{j}_\nu = -|e|c\alpha_\nu$  in Eq. (1) represents the perturbation due to the electric field component  $E_\nu$ . Adopting a fully relativistic formulation to account coherently for the impact of SOC,  $\hat{j}_\nu$  is expressed by the corresponding velocity operator  $\hat{v}_\nu = c\alpha_\nu$ , where  $c$  is the speed of light and  $\alpha_\nu$  is one of the standard  $4 \times 4$  Dirac matrices.<sup>52</sup> The torque operator  $\hat{T}_\mu$  on the other hand represents the change of the magnetization component

$m_\mu$  with time in response to the electric field  $\mathbf{E}$ . Accordingly,  $\hat{T}_\mu$  may be expressed by the partial derivative of the Dirac Hamiltonian  $\mathcal{H}$  with respect to the component  $u_\mu$  of the normalized magnetisation  $\mathbf{m}/|\mathbf{m}|$ :<sup>53</sup>

$$\begin{aligned}\hat{T}_\mu &= \frac{\partial}{\partial u_\mu} \hat{\mathcal{H}} \\ &= \beta \sigma_\mu B_{xc}(\mathbf{r}).\end{aligned}\quad (2)$$

For the second line use has been made of the specific form of  $\hat{\mathcal{H}}$  for a magnetic solid within the framework of local spin density formalism (LSDA) where  $B_{xc}(\mathbf{r})$  stands for the difference in the exchange potential for electrons with spin up and down<sup>54</sup> and  $\sigma_\mu$  is one of the  $4 \times 4$  Pauli spin matrices.<sup>52</sup>

In Eq. (1) the electronic structure is represented in terms of the retarded and advanced Green functions  $G^+(E)$  and  $G^-(E)$ , respectively. Using this approach has the big advantage that one can deal straightforwardly with disordered systems. Considering for example chemical disorder the brackets  $\langle \dots \rangle$  in Eq. (1) stand for the configurational average in a disordered alloy. For the applications presented below relativistic multiple scattering theory was used to determine the Green function.<sup>55,56</sup> The average over alloy configurations was determined by means of the Coherent Potential Approximation (CPA) alloy theory as done in the context of the electrical conductivity,<sup>57,58</sup> spin conductivity<sup>59</sup> and Gilbert damping parameter.<sup>53</sup> This implies in particular that the so-called vertex corrections, that ensure that the proper average  $\langle \hat{T}_\mu G^\pm \hat{j}_\nu G^\pm \rangle$  is taken instead of the simpler one  $\langle \hat{T}_\mu G^\pm \rangle \langle \hat{j}_\nu G^\pm \rangle$ , are included in the calculations.

Expressing the electric field induced torque by means of linear response formalism allows investigating straightforwardly the condition for which the SOT may show up or not. This can be done using a scheme worked out by Kleiner<sup>60</sup> and extended recently by Seemann *et al.*<sup>61</sup> Making use of the behavior of the torque operator  $\hat{T}_\mu$  and of the current density operator  $j_\nu$  under symmetry operations one is led to the relations that restrict the shape of the torkance tensor  $\underline{t}$ :

$$t_{\mu\nu} = \sum_{\kappa\lambda} t_{\kappa\lambda} D(R)_{\kappa\mu} D(R)_{\lambda\nu} \det(R) \quad (3)$$

$$t_{\mu\nu} = - \sum_{\kappa\lambda} t'_{\lambda\kappa} D(R)_{\kappa\mu}^* D(R)_{\lambda\nu}^* \det(R), \quad (4)$$

where  $\underline{D}(R)$  is the  $3 \times 3$  transformation matrix associated with the pure spatial operation  $R$  and  $\det(R)$  is the corresponding determinant of that matrix. In Eq. (3) only unitary pure spatial symmetry operations are considered, while in Eq. (4) anti-unitary operations are considered that involve apart from the spatial operation  $R$  also the time reversal operation. As a consequence Eq. (4) relates the torkance tensor  $\underline{t}$  with the tensor  $\underline{t}'$  that is associated with the effect inverse to the SOT, i.e., Eq. (4) is equivalent to an Onsager relation for  $\underline{t}$ .

Considering Eq. (3) for all symmetry operations of a magnetic point group, the corresponding symmetry-allowed shape of the direct and inverse torkance tensors,  $\underline{t}$  and  $\underline{t}'$ , can be determined. Tables I to VI give the results for all magnetic point groups leading to a non-vanishing torkance tensor. In addition the tensor shapes for electrical and spin conductivity for polarization along the principal axis are given for the respective magnetic Laue groups obtained by adding the spatial inversion operation.<sup>60,61</sup> Naturally, this leads to redundancies since different magnetic point groups have the same magnetic Laue group.

Magnetic symmetry groups that allow for a finite magnetization in general can be subdivided into two categories,<sup>60,61</sup> one without any time-reversal symmetry, neither as an operation on its own nor in combination with a spatial operation, category b) (Table I), the other containing time-reversal only connected with a spatial operation, category c) (Tables II–VI). Naturally, this excludes all magnetic point groups of category a) corresponding to a non-magnetic solid, i.e., that contain time-reversal as separate element.<sup>60,61</sup>

Comparing the results for magnetic point groups of categories b) in Table I and c) in Tables II–VI, one notes that those of the former exhibit identical direct and inverse torkance tensor shapes,  $\underline{t}$  and  $\underline{t}'$ , while for those of the latter the two tensors usually differ in shape but nevertheless are connected to each other. This becomes obvious when looking at Eq. (4): if there was time-reversal as a separate operation, as in a group of category a), the corresponding spatial operation  $R$  would be the identity, and therefore  $t_{\mu\nu} = -t'_{\nu\mu}$  for all tensor elements, i.e., something quite similar to the usual Onsager relations would hold. When there are no time-reversal-connected, i.e., anti-unitary operations in the group, as in category b), Eq. (4) does not apply at all and the shape of  $\underline{t}'$  is given exclusively by Eq. (3) and therefore identical to that of  $\underline{t}$ . For the magnetic point groups of category c), where time-reversal appears only in connection with a spatial operation  $R$ , the shape of  $\underline{t}'$  is determined by  $\underline{D}(R)$ , i.e., the nature of the operation connecting  $\underline{t}$  and  $\underline{t}'$ .

In addition one notices that none of the magnetic point groups listed in Tables I–VI contains the spatial inversion as an element. This central restriction – missing inversion symmetry – has been pointed out before by Manchon and Zhang<sup>2</sup> as well as Garate and MacDonald<sup>3</sup> on the basis of restricted model considerations. This basic requirement is explained here on group-theoretical grounds by the transformation properties of the operators appearing in the linear response expression. The torque operator, represented by the vector product of magnetization and effective magnetic field – both pseudo vectors symmetric under spatial inversion but anti-symmetric under time reversal – hence transforms as time-reversal symmetric pseudo vector, while the electric current density operator as a proper vector is anti-symmetric under both. Therefore the product of the two is both time-reversal- and

magnetic point group	$\underline{t}$	$\underline{t}'$	magnetic Laue group	$\underline{\sigma}$	$\underline{\sigma}^k$
1	$\begin{pmatrix} t_{xx} & t_{xy} & t_{xz} \\ t_{yx} & t_{yy} & t_{yz} \\ t_{zx} & t_{zy} & t_{zz} \end{pmatrix}$	$\begin{pmatrix} t'_{xx} & t'_{xy} & t'_{xz} \\ t'_{yx} & t'_{yy} & t'_{yz} \\ t'_{zx} & t'_{zy} & t'_{zz} \end{pmatrix}$	$\bar{1}$	$\begin{pmatrix} \sigma_{xx} & \sigma_{xy} & \sigma_{xz} \\ \sigma_{yx} & \sigma_{yy} & \sigma_{yz} \\ \sigma_{zx} & \sigma_{zy} & \sigma_{zz} \end{pmatrix}$	$\begin{pmatrix} \sigma_{xx}^z & \sigma_{xy}^z & \sigma_{xz}^z \\ \sigma_{yx}^z & \sigma_{yy}^z & \sigma_{yz}^z \\ \sigma_{zx}^z & \sigma_{zy}^z & \sigma_{zz}^z \end{pmatrix}$
2	$\begin{pmatrix} t_{xx} & 0 & t_{xz} \\ 0 & t_{yy} & 0 \\ t_{zx} & 0 & t_{zz} \end{pmatrix}$	$\begin{pmatrix} t'_{xx} & 0 & t'_{xz} \\ 0 & t'_{yy} & 0 \\ t'_{zx} & 0 & t'_{zz} \end{pmatrix}$	2/m	$\begin{pmatrix} \sigma_{xx} & 0 & \sigma_{xz} \\ 0 & \sigma_{yy} & 0 \\ \sigma_{zx} & 0 & \sigma_{zz} \end{pmatrix}$	$\begin{pmatrix} \sigma_{xx}^y & 0 & \sigma_{xz}^y \\ 0 & \sigma_{yy}^y & 0 \\ \sigma_{zx}^y & 0 & \sigma_{zz}^y \end{pmatrix}$
m	$\begin{pmatrix} 0 & t_{xy} & 0 \\ t_{yx} & 0 & t_{yz} \\ 0 & t_{zy} & 0 \end{pmatrix}$	$\begin{pmatrix} 0 & t'_{xy} & 0 \\ t'_{yx} & 0 & t'_{yz} \\ 0 & t'_{zy} & 0 \end{pmatrix}$	2/m	$\begin{pmatrix} \sigma_{xx} & 0 & \sigma_{xz} \\ 0 & \sigma_{yy} & 0 \\ \sigma_{zx} & 0 & \sigma_{zz} \end{pmatrix}$	$\begin{pmatrix} \sigma_{xx}^y & 0 & \sigma_{xz}^y \\ 0 & \sigma_{yy}^y & 0 \\ \sigma_{zx}^y & 0 & \sigma_{zz}^y \end{pmatrix}$
222	$\begin{pmatrix} t_{xx} & 0 & 0 \\ 0 & t_{yy} & 0 \\ 0 & 0 & t_{zz} \end{pmatrix}$	$\begin{pmatrix} t'_{xx} & 0 & 0 \\ 0 & t'_{yy} & 0 \\ 0 & 0 & t'_{zz} \end{pmatrix}$	mmm	$\begin{pmatrix} \sigma_{xx} & 0 & 0 \\ 0 & \sigma_{yy} & 0 \\ 0 & 0 & \sigma_{zz} \end{pmatrix}$	$\begin{pmatrix} 0 & \sigma_{xy}^z & 0 \\ \sigma_{yx}^z & 0 & 0 \\ 0 & 0 & 0 \end{pmatrix}$
mm2	$\begin{pmatrix} 0 & t_{xy} & 0 \\ t_{yx} & 0 & 0 \\ 0 & 0 & 0 \end{pmatrix}$	$\begin{pmatrix} 0 & t'_{xy} & 0 \\ t'_{yx} & 0 & 0 \\ 0 & 0 & 0 \end{pmatrix}$	mmm	$\begin{pmatrix} \sigma_{xx} & 0 & 0 \\ 0 & \sigma_{yy} & 0 \\ 0 & 0 & \sigma_{zz} \end{pmatrix}$	$\begin{pmatrix} 0 & \sigma_{xy}^z & 0 \\ \sigma_{yx}^z & 0 & 0 \\ 0 & 0 & 0 \end{pmatrix}$
4	$\begin{pmatrix} t_{xx} & t_{xy} & 0 \\ -t_{xy} & t_{xx} & 0 \\ 0 & 0 & t_{zz} \end{pmatrix}$	$\begin{pmatrix} t'_{xx} & t'_{xy} & 0 \\ -t'_{xy} & t'_{xx} & 0 \\ 0 & 0 & t'_{zz} \end{pmatrix}$	4/m	$\begin{pmatrix} \sigma_{xx} & \sigma_{xy} & 0 \\ -\sigma_{xy} & \sigma_{xx} & 0 \\ 0 & 0 & \sigma_{zz} \end{pmatrix}$	$\begin{pmatrix} \sigma_{xx}^z & \sigma_{xy}^z & 0 \\ -\sigma_{xy}^z & \sigma_{xx}^z & 0 \\ 0 & 0 & \sigma_{zz}^z \end{pmatrix}$
$\bar{4}$	$\begin{pmatrix} t_{xx} & t_{xy} & 0 \\ t_{xy} & -t_{xx} & 0 \\ 0 & 0 & 0 \end{pmatrix}$	$\begin{pmatrix} t'_{xx} & t'_{xy} & 0 \\ t'_{xy} & -t'_{xx} & 0 \\ 0 & 0 & 0 \end{pmatrix}$	4/m	$\begin{pmatrix} \sigma_{xx} & \sigma_{xy} & 0 \\ -\sigma_{xy} & \sigma_{xx} & 0 \\ 0 & 0 & \sigma_{zz} \end{pmatrix}$	$\begin{pmatrix} \sigma_{xx}^z & \sigma_{xy}^z & 0 \\ -\sigma_{xy}^z & \sigma_{xx}^z & 0 \\ 0 & 0 & \sigma_{zz}^z \end{pmatrix}$
422	$\begin{pmatrix} t_{xx} & 0 & 0 \\ 0 & t_{xx} & 0 \\ 0 & 0 & t_{zz} \end{pmatrix}$	$\begin{pmatrix} t'_{xx} & 0 & 0 \\ 0 & t'_{xx} & 0 \\ 0 & 0 & t'_{zz} \end{pmatrix}$	4/mmm	$\begin{pmatrix} \sigma_{xx} & 0 & 0 \\ 0 & \sigma_{xx} & 0 \\ 0 & 0 & \sigma_{zz} \end{pmatrix}$	$\begin{pmatrix} 0 & \sigma_{xy}^z & 0 \\ -\sigma_{xy}^z & 0 & 0 \\ 0 & 0 & 0 \end{pmatrix}$
4mm	$\begin{pmatrix} 0 & t_{xy} & 0 \\ -t_{xy} & 0 & 0 \\ 0 & 0 & 0 \end{pmatrix}$	$\begin{pmatrix} 0 & t'_{xy} & 0 \\ -t'_{xy} & 0 & 0 \\ 0 & 0 & 0 \end{pmatrix}$	4/mmm	$\begin{pmatrix} \sigma_{xx} & 0 & 0 \\ 0 & \sigma_{xx} & 0 \\ 0 & 0 & \sigma_{zz} \end{pmatrix}$	$\begin{pmatrix} 0 & \sigma_{xy}^z & 0 \\ -\sigma_{xy}^z & 0 & 0 \\ 0 & 0 & 0 \end{pmatrix}$
$\bar{4}2m$	$\begin{pmatrix} t_{xx} & 0 & 0 \\ 0 & -t_{xx} & 0 \\ 0 & 0 & 0 \end{pmatrix}$	$\begin{pmatrix} t'_{xx} & 0 & 0 \\ 0 & -t'_{xx} & 0 \\ 0 & 0 & 0 \end{pmatrix}$	4/mmm	$\begin{pmatrix} \sigma_{xx} & 0 & 0 \\ 0 & \sigma_{xx} & 0 \\ 0 & 0 & \sigma_{zz} \end{pmatrix}$	$\begin{pmatrix} 0 & \sigma_{xy}^z & 0 \\ -\sigma_{xy}^z & 0 & 0 \\ 0 & 0 & 0 \end{pmatrix}$
3	$\begin{pmatrix} t_{xx} & t_{xy} & 0 \\ -t_{xy} & t_{xx} & 0 \\ 0 & 0 & t_{zz} \end{pmatrix}$	$\begin{pmatrix} t'_{xx} & t'_{xy} & 0 \\ -t'_{xy} & t'_{xx} & 0 \\ 0 & 0 & t'_{zz} \end{pmatrix}$	$\bar{3}$	$\begin{pmatrix} \sigma_{xx} & \sigma_{xy} & 0 \\ -\sigma_{xy} & \sigma_{xx} & 0 \\ 0 & 0 & \sigma_{zz} \end{pmatrix}$	$\begin{pmatrix} \sigma_{xx}^z & \sigma_{xy}^z & 0 \\ -\sigma_{xy}^z & \sigma_{xx}^z & 0 \\ 0 & 0 & \sigma_{zz}^z \end{pmatrix}$
312	$\begin{pmatrix} t_{xx} & 0 & 0 \\ 0 & t_{xx} & 0 \\ 0 & 0 & t_{zz} \end{pmatrix}$	$\begin{pmatrix} t'_{xx} & 0 & 0 \\ 0 & t'_{xx} & 0 \\ 0 & 0 & t'_{zz} \end{pmatrix}$	$\bar{3}1m$	$\begin{pmatrix} \sigma_{xx} & 0 & 0 \\ 0 & \sigma_{xx} & 0 \\ 0 & 0 & \sigma_{zz} \end{pmatrix}$	$\begin{pmatrix} 0 & \sigma_{xy}^z & 0 \\ -\sigma_{xy}^z & 0 & 0 \\ 0 & 0 & 0 \end{pmatrix}$
31m	$\begin{pmatrix} 0 & t_{xy} & 0 \\ -t_{xy} & 0 & 0 \\ 0 & 0 & 0 \end{pmatrix}$	$\begin{pmatrix} 0 & t'_{xy} & 0 \\ -t'_{xy} & 0 & 0 \\ 0 & 0 & 0 \end{pmatrix}$	$\bar{3}1m$	$\begin{pmatrix} \sigma_{xx} & 0 & 0 \\ 0 & \sigma_{xx} & 0 \\ 0 & 0 & \sigma_{zz} \end{pmatrix}$	$\begin{pmatrix} 0 & \sigma_{xy}^z & 0 \\ -\sigma_{xy}^z & 0 & 0 \\ 0 & 0 & 0 \end{pmatrix}$
6	$\begin{pmatrix} t_{xx} & t_{xy} & 0 \\ -t_{xy} & t_{xx} & 0 \\ 0 & 0 & t_{zz} \end{pmatrix}$	$\begin{pmatrix} t'_{xx} & t'_{xy} & 0 \\ -t'_{xy} & t'_{xx} & 0 \\ 0 & 0 & t'_{zz} \end{pmatrix}$	6/m	$\begin{pmatrix} \sigma_{xx} & \sigma_{xy} & 0 \\ -\sigma_{xy} & \sigma_{xx} & 0 \\ 0 & 0 & \sigma_{zz} \end{pmatrix}$	$\begin{pmatrix} \sigma_{xx}^z & \sigma_{xy}^z & 0 \\ -\sigma_{xy}^z & \sigma_{xx}^z & 0 \\ 0 & 0 & \sigma_{zz}^z \end{pmatrix}$
622	$\begin{pmatrix} t_{xx} & 0 & 0 \\ 0 & t_{xx} & 0 \\ 0 & 0 & t_{zz} \end{pmatrix}$	$\begin{pmatrix} t'_{xx} & 0 & 0 \\ 0 & t'_{xx} & 0 \\ 0 & 0 & t'_{zz} \end{pmatrix}$	6/mmm	$\begin{pmatrix} \sigma_{xx} & 0 & 0 \\ 0 & \sigma_{xx} & 0 \\ 0 & 0 & \sigma_{zz} \end{pmatrix}$	$\begin{pmatrix} 0 & \sigma_{xy}^z & 0 \\ -\sigma_{xy}^z & 0 & 0 \\ 0 & 0 & 0 \end{pmatrix}$
6mm	$\begin{pmatrix} 0 & t_{xy} & 0 \\ -t_{xy} & 0 & 0 \\ 0 & 0 & 0 \end{pmatrix}$	$\begin{pmatrix} 0 & t'_{xy} & 0 \\ -t'_{xy} & 0 & 0 \\ 0 & 0 & 0 \end{pmatrix}$	6/mmm	$\begin{pmatrix} \sigma_{xx} & 0 & 0 \\ 0 & \sigma_{xx} & 0 \\ 0 & 0 & \sigma_{zz} \end{pmatrix}$	$\begin{pmatrix} 0 & \sigma_{xy}^z & 0 \\ -\sigma_{xy}^z & 0 & 0 \\ 0 & 0 & 0 \end{pmatrix}$
23	$\begin{pmatrix} t_{xx} & 0 & 0 \\ 0 & t_{xx} & 0 \\ 0 & 0 & t_{xx} \end{pmatrix}$	$\begin{pmatrix} t'_{xx} & 0 & 0 \\ 0 & t'_{xx} & 0 \\ 0 & 0 & t'_{xx} \end{pmatrix}$	$m\bar{3}$	$\begin{pmatrix} \sigma_{xx} & 0 & 0 \\ 0 & \sigma_{xx} & 0 \\ 0 & 0 & \sigma_{xx} \end{pmatrix}$	$\begin{pmatrix} 0 & \sigma_{xy}^z & 0 \\ xzy & 0 & 0 \\ 0 & 0 & 0 \end{pmatrix}$
432	$\begin{pmatrix} t_{xx} & 0 & 0 \\ 0 & t_{xx} & 0 \\ 0 & 0 & t_{xx} \end{pmatrix}$	$\begin{pmatrix} t'_{xx} & 0 & 0 \\ 0 & t'_{xx} & 0 \\ 0 & 0 & t'_{xx} \end{pmatrix}$	$m\bar{3}m$	$\begin{pmatrix} \sigma_{xx} & 0 & 0 \\ 0 & \sigma_{xx} & 0 \\ 0 & 0 & \sigma_{xx} \end{pmatrix}$	$\begin{pmatrix} 0 & \sigma_{xy}^z & 0 \\ -\sigma_{xy}^z & 0 & 0 \\ 0 & 0 & 0 \end{pmatrix}$

Table I. Shape of the direct and inverse torquance tensors,  $\underline{t}$  and  $\underline{t}'$ , for all magnetic point groups of category b). Note that since these do not contain time-reversal, neither as an element on its own nor in combination with a spatial operation, the two tensors are unconnected and identical in shape. The third and fourth columns show the electrical conductivity tensor  $\underline{\sigma}$  and the spin conductivity tensor  $\underline{\sigma}^k$  for polarization along the principal axis  $k$ , respectively, for the corresponding magnetic Laue groups. See Ref. 61 for the two remaining polarization directions and further details on conventions and notation.

magnetic point group	$\underline{t}$	$\underline{t}'$	magnetic Laue group	$\underline{\sigma}$	$\underline{\sigma}^k$
$\bar{1}'$	$\begin{pmatrix} t_{xx} & t_{xy} & t_{xz} \\ t_{yx} & t_{yy} & t_{yz} \\ t_{zx} & t_{zy} & t_{zz} \end{pmatrix}$	$\begin{pmatrix} t_{xx} & t_{yx} & t_{zx} \\ t_{xy} & t_{yy} & t_{zy} \\ t_{xz} & t_{yz} & t_{zz} \end{pmatrix}$	$\bar{1}1'$	$\begin{pmatrix} \sigma_{xx} & \sigma_{xy} & \sigma_{xz} \\ \sigma_{xy} & \sigma_{yy} & \sigma_{yz} \\ \sigma_{xz} & \sigma_{yz} & \sigma_{zz} \end{pmatrix}$	$\begin{pmatrix} \sigma_{xx}^z & \sigma_{xy}^z & \sigma_{xz}^z \\ \sigma_{yx}^z & \sigma_{yy}^z & \sigma_{yz}^z \\ \sigma_{zx}^z & \sigma_{zy}^z & \sigma_{zz}^z \end{pmatrix}$
$2'$	$\begin{pmatrix} t_{xx} & t_{xy} & t_{xz} \\ t_{yx} & t_{yy} & t_{yz} \\ t_{zx} & t_{zy} & t_{zz} \end{pmatrix}$	$\begin{pmatrix} -t_{xx} & t_{yx} & -t_{zx} \\ t_{xy} & -t_{yy} & t_{zy} \\ -t_{xz} & t_{yz} & -t_{zz} \end{pmatrix}$	$2'/m'$	$\begin{pmatrix} \sigma_{xx} & \sigma_{xy} & \sigma_{xz} \\ -\sigma_{xy} & \sigma_{yy} & \sigma_{yz} \\ \sigma_{xz} & -\sigma_{yz} & \sigma_{zz} \end{pmatrix}$	$\begin{pmatrix} \sigma_{xx}^y & \sigma_{xy}^y & \sigma_{xz}^y \\ \sigma_{yx}^y & \sigma_{yy}^y & \sigma_{yz}^y \\ \sigma_{zx}^y & \sigma_{zy}^y & \sigma_{zz}^y \end{pmatrix}$
$m'$	$\begin{pmatrix} t_{xx} & t_{xy} & t_{xz} \\ t_{yx} & t_{yy} & t_{yz} \\ t_{zx} & t_{zy} & t_{zz} \end{pmatrix}$	$\begin{pmatrix} t_{xx} & -t_{yx} & t_{zx} \\ -t_{xy} & t_{yy} & -t_{zy} \\ t_{xz} & -t_{yz} & t_{zz} \end{pmatrix}$	$2'/m'$	$\begin{pmatrix} \sigma_{xx} & \sigma_{xy} & \sigma_{xz} \\ -\sigma_{xy} & \sigma_{yy} & \sigma_{yz} \\ \sigma_{xz} & -\sigma_{yz} & \sigma_{zz} \end{pmatrix}$	$\begin{pmatrix} \sigma_{xx}^y & \sigma_{xy}^y & \sigma_{xz}^y \\ \sigma_{yx}^y & \sigma_{yy}^y & \sigma_{yz}^y \\ \sigma_{zx}^y & \sigma_{zy}^y & \sigma_{zz}^y \end{pmatrix}$
$2/m'$	$\begin{pmatrix} t_{xx} & 0 & t_{xz} \\ 0 & t_{yy} & 0 \\ t_{zx} & 0 & t_{zz} \end{pmatrix}$	$\begin{pmatrix} t_{xx} & 0 & t_{zx} \\ 0 & t_{yy} & 0 \\ t_{xz} & 0 & t_{zz} \end{pmatrix}$	$2/m1'$	$\begin{pmatrix} \sigma_{xx} & 0 & \sigma_{xz} \\ 0 & \sigma_{yy} & 0 \\ \sigma_{xz} & 0 & \sigma_{zz} \end{pmatrix}$	$\begin{pmatrix} \sigma_{xx}^y & 0 & \sigma_{xz}^y \\ 0 & \sigma_{yy}^y & 0 \\ \sigma_{zx}^y & 0 & \sigma_{zz}^y \end{pmatrix}$
$2'/m$	$\begin{pmatrix} 0 & t_{xy} & 0 \\ t_{yx} & 0 & t_{yz} \\ 0 & t_{zy} & 0 \end{pmatrix}$	$\begin{pmatrix} 0 & t_{yx} & 0 \\ t_{xy} & 0 & t_{zy} \\ 0 & t_{yz} & 0 \end{pmatrix}$	$2/m1'$	$\begin{pmatrix} \sigma_{xx} & 0 & \sigma_{xz} \\ 0 & \sigma_{yy} & 0 \\ \sigma_{xz} & 0 & \sigma_{zz} \end{pmatrix}$	$\begin{pmatrix} \sigma_{xx}^y & 0 & \sigma_{xz}^y \\ 0 & \sigma_{yy}^y & 0 \\ \sigma_{zx}^y & 0 & \sigma_{zz}^y \end{pmatrix}$
$2'2'2$	$\begin{pmatrix} t_{xx} & t_{xy} & 0 \\ t_{yx} & t_{yy} & 0 \\ 0 & 0 & t_{zz} \end{pmatrix}$	$\begin{pmatrix} -t_{xx} & t_{yx} & 0 \\ t_{xy} & -t_{yy} & 0 \\ 0 & 0 & -t_{zz} \end{pmatrix}$	$m'm'm$	$\begin{pmatrix} \sigma_{xx} & \sigma_{xy} & 0 \\ -\sigma_{xy} & \sigma_{yy} & 0 \\ 0 & 0 & \sigma_{zz} \end{pmatrix}$	$\begin{pmatrix} \sigma_{xx}^z & \sigma_{xy}^z & 0 \\ \sigma_{yx}^z & \sigma_{yy}^z & 0 \\ 0 & 0 & \sigma_{zz}^z \end{pmatrix}$
$m'm'2$	$\begin{pmatrix} t_{xx} & t_{xy} & 0 \\ t_{yx} & t_{yy} & 0 \\ 0 & 0 & t_{zz} \end{pmatrix}$	$\begin{pmatrix} t_{xx} & -t_{yx} & 0 \\ -t_{xy} & t_{yy} & 0 \\ 0 & 0 & t_{zz} \end{pmatrix}$	$m'm'm$	$\begin{pmatrix} \sigma_{xx} & \sigma_{xy} & 0 \\ -\sigma_{xy} & \sigma_{yy} & 0 \\ 0 & 0 & \sigma_{zz} \end{pmatrix}$	$\begin{pmatrix} \sigma_{xx}^z & \sigma_{xy}^z & 0 \\ \sigma_{yx}^z & \sigma_{yy}^z & 0 \\ 0 & 0 & \sigma_{zz}^z \end{pmatrix}$
$m'm'2'$	$\begin{pmatrix} 0 & t_{xy} & 0 \\ t_{yx} & 0 & t_{yz} \\ 0 & t_{zy} & 0 \end{pmatrix}$	$\begin{pmatrix} 0 & -t_{yx} & 0 \\ -t_{xy} & 0 & t_{zy} \\ 0 & t_{yz} & 0 \end{pmatrix}$	$m'm'm$	$\begin{pmatrix} \sigma_{xx} & 0 & \sigma_{xz} \\ 0 & \sigma_{yy} & 0 \\ -\sigma_{xz} & 0 & \sigma_{zz} \end{pmatrix}$	$\begin{pmatrix} 0 & \sigma_{xy}^z & 0 \\ \sigma_{yx}^z & 0 & \sigma_{yz}^z \\ 0 & \sigma_{zy}^z & 0 \end{pmatrix}$
$m'm'm'$	$\begin{pmatrix} t_{xx} & 0 & 0 \\ 0 & t_{yy} & 0 \\ 0 & 0 & t_{zz} \end{pmatrix}$	$\begin{pmatrix} t_{xx} & 0 & 0 \\ 0 & t_{yy} & 0 \\ 0 & 0 & t_{zz} \end{pmatrix}$	$mmm1'$	$\begin{pmatrix} \sigma_{xx} & 0 & 0 \\ 0 & \sigma_{yy} & 0 \\ 0 & 0 & \sigma_{zz} \end{pmatrix}$	$\begin{pmatrix} 0 & \sigma_{xy}^z & 0 \\ \sigma_{yx}^z & 0 & 0 \\ 0 & 0 & 0 \end{pmatrix}$
$m'mm$	$\begin{pmatrix} 0 & 0 & 0 \\ 0 & 0 & t_{yz} \\ 0 & t_{zy} & 0 \end{pmatrix}$	$\begin{pmatrix} 0 & 0 & 0 \\ 0 & 0 & t_{zy} \\ 0 & t_{yz} & 0 \end{pmatrix}$	$mmm1'$	$\begin{pmatrix} \sigma_{xx} & 0 & 0 \\ 0 & \sigma_{yy} & 0 \\ 0 & 0 & \sigma_{zz} \end{pmatrix}$	$\begin{pmatrix} 0 & \sigma_{xy}^z & 0 \\ \sigma_{yx}^z & 0 & 0 \\ 0 & 0 & 0 \end{pmatrix}$

Table II. Shape of the direct and inverse torkance tensors,  $\underline{t}$  and  $\underline{t}'$ , for magnetic point groups of category c). Note that the two tensors usually differ in shape, depending on which spatial operation is combined with time-reversal. The third and fourth columns show the electrical conductivity tensor  $\underline{\sigma}$  and the spin conductivity tensor  $\underline{\sigma}^k$  for polarization along the principal axis  $k$ , respectively, for the corresponding magnetic Laue groups. See Ref. 61 for the two remaining polarization directions and further details on conventions and notation. This Table contains only groups with a principal axis of order  $O(k) \leq 2$  and is continued in Tables III–VI.

inversion anti-symmetric. Correspondingly, the shapes of direct and inverse torkance tensors are determined by the magnetic point group of a solid, in contrast for example to the electrical conductivity and thermoelectric tensors,<sup>60</sup> as well as to the spin conductivity tensor.<sup>61</sup>

Since the operators for electric and heat current densities transform identical under all space-time symmetry operations relevant for solids,<sup>60,61</sup> the tensor shapes will stay unaltered when the electric field is replaced by a temperature gradient. In other words, the shapes given here apply also for the direct and inverse thermal spin-orbit torque effect discussed recently by Géronton *et al.*<sup>47</sup> and Freimuth *et al.*<sup>48</sup>.

Finally, it should be mentioned that the results for the torkance tensors presented in Tables I–VI have been independently checked for a number of systems, including  $m'm'm$ ,  $4/mm'm'$ ,  $6/mm'm'$ ,  $\bar{3}m'$  with vanishing torkance and  $1$ ,  $m'$ ,  $m'm'2$ ,  $\bar{4}2'm'$ ,  $3m'$ ,  $\bar{6}'2m'$ ,  $6/m'm'm'$  with finite torkance, by numerical calculations using the implementation described above.

### III. RESULTS

To investigate the impact of chemical disorder and the ability to tailor the torkance via the alloy composition the multilayer system Pt|Fe<sub>x</sub>Co<sub>1-x</sub>|Cu has been investigated over the full range of concentration  $x$ . Fig. 1 shows the hexagonal structure of the model system for which a stacking of fcc (111)-like atomic planes along the  $z$  axis has been assumed.

To examine the connection of the torkance with other related response quantities we calculated the electrical and spin conductivity tensors in addition. Replacing the torque operator  $\hat{T}_\mu$  in Eq. (1) by the operator  $\hat{j}_\mu$  one gets, apart from some constants, the corresponding expressions for the electrical conductivity tensor  $\underline{\sigma}$ . From this one can see immediately that the longitudinal conductivities  $\sigma_{ii}$  are connected only with the first Fermi surface term in Eq. (1), accordingly they are determined for  $T = 0$  K by the electronic structure at the Fermi energy  $E_F$  while the second Fermi sea term vanishes. Due to the magnetic Laue group ( $\bar{3}m'$ ) of the investig-

magnetic point group	$\underline{t}$	$\underline{t}'$	magnetic Laue group	$\underline{\sigma}$	$\underline{\sigma}^k$
$4'$	$\begin{pmatrix} t_{xx} & t_{xy} & 0 \\ t_{yx} & t_{yy} & 0 \\ 0 & 0 & t_{zz} \end{pmatrix}$	$\begin{pmatrix} -t_{yy} & t_{xy} & 0 \\ t_{yx} & -t_{xx} & 0 \\ 0 & 0 & -t_{zz} \end{pmatrix}$	$4'/m$	$\begin{pmatrix} \sigma_{xx} & 0 & 0 \\ 0 & \sigma_{xx} & 0 \\ 0 & 0 & \sigma_{zz} \end{pmatrix}$	$\begin{pmatrix} \sigma_{xx}^z & \sigma_{xy}^z & 0 \\ \sigma_{yx}^z & \sigma_{yy}^z & 0 \\ 0 & 0 & \sigma_{zz}^z \end{pmatrix}$
$\bar{4}'$	$\begin{pmatrix} t_{xx} & t_{xy} & 0 \\ t_{yx} & t_{yy} & 0 \\ 0 & 0 & t_{zz} \end{pmatrix}$	$\begin{pmatrix} t_{yy} & -t_{xy} & 0 \\ -t_{yx} & t_{xx} & 0 \\ 0 & 0 & t_{zz} \end{pmatrix}$	$4'/m$	$\begin{pmatrix} \sigma_{xx} & 0 & 0 \\ 0 & \sigma_{xx} & 0 \\ 0 & 0 & \sigma_{zz} \end{pmatrix}$	$\begin{pmatrix} \sigma_{xx}^z & \sigma_{xy}^z & 0 \\ \sigma_{yx}^z & \sigma_{yy}^z & 0 \\ 0 & 0 & \sigma_{zz}^z \end{pmatrix}$
$4/m'$	$\begin{pmatrix} t_{xx} & t_{xy} & 0 \\ -t_{xy} & t_{xx} & 0 \\ 0 & 0 & t_{zz} \end{pmatrix}$	$\begin{pmatrix} t_{xx} & -t_{xy} & 0 \\ t_{xy} & t_{xx} & 0 \\ 0 & 0 & t_{zz} \end{pmatrix}$	$4/m1'$	$\begin{pmatrix} \sigma_{xx} & 0 & 0 \\ 0 & \sigma_{xx} & 0 \\ 0 & 0 & \sigma_{zz} \end{pmatrix}$	$\begin{pmatrix} \sigma_{xx}^z & \sigma_{xy}^z & 0 \\ -\sigma_{xy}^z & \sigma_{xx}^z & 0 \\ 0 & 0 & \sigma_{zz}^z \end{pmatrix}$
$4'/m'$	$\begin{pmatrix} t_{xx} & t_{xy} & 0 \\ t_{xy} & -t_{xx} & 0 \\ 0 & 0 & 0 \end{pmatrix}$	$\begin{pmatrix} t_{xx} & t_{xy} & 0 \\ t_{xy} & -t_{xx} & 0 \\ 0 & 0 & 0 \end{pmatrix}$	$4/m1'$	$\begin{pmatrix} \sigma_{xx} & 0 & 0 \\ 0 & \sigma_{xx} & 0 \\ 0 & 0 & \sigma_{zz} \end{pmatrix}$	$\begin{pmatrix} \sigma_{xx}^z & \sigma_{xy}^z & 0 \\ -\sigma_{xy}^z & \sigma_{xx}^z & 0 \\ 0 & 0 & \sigma_{zz}^z \end{pmatrix}$
$4'22'$	$\begin{pmatrix} t_{xx} & 0 & 0 \\ 0 & t_{yy} & 0 \\ 0 & 0 & t_{zz} \end{pmatrix}$	$\begin{pmatrix} -t_{yy} & 0 & 0 \\ 0 & -t_{xx} & 0 \\ 0 & 0 & -t_{zz} \end{pmatrix}$	$4'/mmm'$	$\begin{pmatrix} \sigma_{xx} & 0 & 0 \\ 0 & \sigma_{xx} & 0 \\ 0 & 0 & \sigma_{zz} \end{pmatrix}$	$\begin{pmatrix} 0 & \sigma_{xy}^z & 0 \\ \sigma_{yx}^z & 0 & 0 \\ 0 & 0 & 0 \end{pmatrix}$
$42'2'$	$\begin{pmatrix} t_{xx} & t_{xy} & 0 \\ -t_{xy} & t_{xx} & 0 \\ 0 & 0 & t_{zz} \end{pmatrix}$	$\begin{pmatrix} -t_{xx} & -t_{xy} & 0 \\ t_{xy} & -t_{xx} & 0 \\ 0 & 0 & -t_{zz} \end{pmatrix}$	$4/mm'm'$	$\begin{pmatrix} \sigma_{xx} & \sigma_{xy} & 0 \\ -\sigma_{xy} & \sigma_{xx} & 0 \\ 0 & 0 & \sigma_{zz} \end{pmatrix}$	$\begin{pmatrix} \sigma_{xx}^z & \sigma_{xy}^z & 0 \\ -\sigma_{xy}^z & \sigma_{xx}^z & 0 \\ 0 & 0 & \sigma_{zz}^z \end{pmatrix}$
$4'mm'$	$\begin{pmatrix} 0 & t_{xy} & 0 \\ t_{yx} & 0 & 0 \\ 0 & 0 & 0 \end{pmatrix}$	$\begin{pmatrix} 0 & t_{xy} & 0 \\ t_{yx} & 0 & 0 \\ 0 & 0 & 0 \end{pmatrix}$	$4'/mmm'$	$\begin{pmatrix} \sigma_{xx} & 0 & 0 \\ 0 & \sigma_{xx} & 0 \\ 0 & 0 & \sigma_{zz} \end{pmatrix}$	$\begin{pmatrix} 0 & \sigma_{xy}^z & 0 \\ \sigma_{yx}^z & 0 & 0 \\ 0 & 0 & 0 \end{pmatrix}$
$4m'm'$	$\begin{pmatrix} t_{xx} & t_{xy} & 0 \\ -t_{xy} & t_{xx} & 0 \\ 0 & 0 & t_{zz} \end{pmatrix}$	$\begin{pmatrix} t_{xx} & t_{xy} & 0 \\ -t_{xy} & t_{xx} & 0 \\ 0 & 0 & t_{zz} \end{pmatrix}$	$4/mm'm'$	$\begin{pmatrix} \sigma_{xx} & \sigma_{xy} & 0 \\ -\sigma_{xy} & \sigma_{xx} & 0 \\ 0 & 0 & \sigma_{zz} \end{pmatrix}$	$\begin{pmatrix} \sigma_{xx}^z & \sigma_{xy}^z & 0 \\ -\sigma_{xy}^z & \sigma_{xx}^z & 0 \\ 0 & 0 & \sigma_{zz}^z \end{pmatrix}$
$\bar{4}'2m'$	$\begin{pmatrix} t_{xx} & 0 & 0 \\ 0 & t_{yy} & 0 \\ 0 & 0 & t_{zz} \end{pmatrix}$	$\begin{pmatrix} t_{yy} & 0 & 0 \\ 0 & t_{xx} & 0 \\ 0 & 0 & t_{zz} \end{pmatrix}$	$4'/mmm'$	$\begin{pmatrix} \sigma_{xx} & 0 & 0 \\ 0 & \sigma_{xx} & 0 \\ 0 & 0 & \sigma_{zz} \end{pmatrix}$	$\begin{pmatrix} 0 & \sigma_{xy}^z & 0 \\ \sigma_{yx}^z & 0 & 0 \\ 0 & 0 & 0 \end{pmatrix}$
$\bar{4}'m2'$	$\begin{pmatrix} 0 & t_{xy} & 0 \\ t_{yx} & 0 & 0 \\ 0 & 0 & 0 \end{pmatrix}$	$\begin{pmatrix} 0 & -t_{xy} & 0 \\ -t_{yx} & 0 & 0 \\ 0 & 0 & 0 \end{pmatrix}$	$4'/mmm'$	$\begin{pmatrix} \sigma_{xx} & 0 & 0 \\ 0 & \sigma_{xx} & 0 \\ 0 & 0 & \sigma_{zz} \end{pmatrix}$	$\begin{pmatrix} 0 & \sigma_{xy}^z & 0 \\ \sigma_{yx}^z & 0 & 0 \\ 0 & 0 & 0 \end{pmatrix}$
$\bar{4}2'm'$	$\begin{pmatrix} t_{xx} & t_{xy} & 0 \\ t_{xy} & -t_{xx} & 0 \\ 0 & 0 & 0 \end{pmatrix}$	$\begin{pmatrix} -t_{xx} & t_{xy} & 0 \\ t_{xy} & t_{xx} & 0 \\ 0 & 0 & 0 \end{pmatrix}$	$4/mm'm'$	$\begin{pmatrix} \sigma_{xx} & \sigma_{xy} & 0 \\ -\sigma_{xy} & \sigma_{xx} & 0 \\ 0 & 0 & \sigma_{zz} \end{pmatrix}$	$\begin{pmatrix} \sigma_{xx}^z & \sigma_{xy}^z & 0 \\ -\sigma_{xy}^z & \sigma_{xx}^z & 0 \\ 0 & 0 & \sigma_{zz}^z \end{pmatrix}$
$4/m'm'm'$	$\begin{pmatrix} t_{xx} & 0 & 0 \\ 0 & t_{xx} & 0 \\ 0 & 0 & t_{zz} \end{pmatrix}$	$\begin{pmatrix} t_{xx} & 0 & 0 \\ 0 & t_{xx} & 0 \\ 0 & 0 & t_{zz} \end{pmatrix}$	$4/mmm1'$	$\begin{pmatrix} \sigma_{xx} & 0 & 0 \\ 0 & \sigma_{xx} & 0 \\ 0 & 0 & \sigma_{zz} \end{pmatrix}$	$\begin{pmatrix} 0 & \sigma_{xy}^z & 0 \\ -\sigma_{xy}^z & 0 & 0 \\ 0 & 0 & 0 \end{pmatrix}$
$4/m'mm$	$\begin{pmatrix} 0 & t_{xy} & 0 \\ -t_{xy} & 0 & 0 \\ 0 & 0 & 0 \end{pmatrix}$	$\begin{pmatrix} 0 & -t_{xy} & 0 \\ t_{xy} & 0 & 0 \\ 0 & 0 & 0 \end{pmatrix}$	$4/mmm1'$	$\begin{pmatrix} \sigma_{xx} & 0 & 0 \\ 0 & \sigma_{xx} & 0 \\ 0 & 0 & \sigma_{zz} \end{pmatrix}$	$\begin{pmatrix} 0 & \sigma_{xy}^z & 0 \\ -\sigma_{xy}^z & 0 & 0 \\ 0 & 0 & 0 \end{pmatrix}$
$4'/m'm'm$	$\begin{pmatrix} t_{xx} & 0 & 0 \\ 0 & -t_{xx} & 0 \\ 0 & 0 & 0 \end{pmatrix}$	$\begin{pmatrix} t_{xx} & 0 & 0 \\ 0 & -t_{xx} & 0 \\ 0 & 0 & 0 \end{pmatrix}$	$4/mmm1'$	$\begin{pmatrix} \sigma_{xx} & 0 & 0 \\ 0 & \sigma_{xx} & 0 \\ 0 & 0 & \sigma_{zz} \end{pmatrix}$	$\begin{pmatrix} 0 & \sigma_{xy}^z & 0 \\ -\sigma_{xy}^z & 0 & 0 \\ 0 & 0 & 0 \end{pmatrix}$

Table III. Table II continued for tetragonal groups with  $O(k) = 4$ .

ated system the conductivity tensor  $\underline{\sigma}$  has only the non-vanishing elements  $\sigma_{xx} = \sigma_{yy} \neq \sigma_{zz}$  and  $\sigma_{xy} = -\sigma_{yx}$ ,<sup>61</sup> i.e., the well-known shape of ferromagnetic systems with a principal axis  $k$  of order  $O(k) \geq 3$  and neither additional purely spatial rotation axes perpendicular to it, nor vertical mirror planes. The corresponding results for Pt|Fe<sub>x</sub>Co<sub>1-x</sub>|Cu are shown in Fig. 2 as a function of the concentration  $x$ . As to be expected for  $T = 0$  K one finds a divergent behavior for the longitudinal conductivities  $\sigma_{xx}$  and  $\sigma_{zz}$  in the dilute regime, i.e., when  $x$  goes to 0 or 1, respectively. In both cases the variation with  $x$  is rather symmetric around the composition  $x = 0.5$  as the two alloying components, Fe and Co, respectively, do not differ too much concerning their electronic properties in this fcc (111)-like structure. Apart from this

general behavior one notes that one has  $\sigma_{xx} > \sigma_{zz}$  for all concentrations. This is due to the simple fact that for  $\sigma_{xx}$  one has electronic transport parallel to the atomic layers while  $\sigma_{zz}$  implies transport perpendicular to the layers, the finite conductivity is not only because of the chemical disorder in the Fe-Co layers but in addition due to a strong geometrical confinement and corresponding interface scattering. Fig. 2 (top) shows also the conductivity  $\sigma_{xx}$  and  $\sigma_{zz}$  calculated without the vertex corrections. As one can see, this restriction hardly changes the numerical results. This finding is very typical for transition metal systems with a high density of states at the Fermi energy implying a short mean free path length.<sup>62</sup> In contrast to the longitudinal conductivity  $\sigma_{ii}$  the transverse conductivity  $\sigma_{xy}$  has contributions from the Fermi

magnetic point group	$\underline{t}$	$\underline{t}'$	magnetic Laue group	$\underline{\sigma}$	$\underline{\sigma}^k$
$\bar{3}'$	$\begin{pmatrix} t_{xx} & t_{xy} & 0 \\ -t_{xy} & t_{xx} & 0 \\ 0 & 0 & t_{zz} \end{pmatrix}$	$\begin{pmatrix} t_{xx} - t_{xy} & 0 \\ t_{xy} & t_{xx} & 0 \\ 0 & 0 & t_{zz} \end{pmatrix}$	$\bar{3}1'$	$\begin{pmatrix} \sigma_{xx} & 0 & 0 \\ 0 & \sigma_{xx} & 0 \\ 0 & 0 & \sigma_{zz} \end{pmatrix}$	$\begin{pmatrix} \sigma_{xx}^z & \sigma_{xy}^z & 0 \\ -\sigma_{xy}^z & \sigma_{xx}^z & 0 \\ 0 & 0 & \sigma_{zz}^z \end{pmatrix}$
$312'$	$\begin{pmatrix} t_{xx} & t_{xy} & 0 \\ -t_{xy} & t_{xx} & 0 \\ 0 & 0 & t_{zz} \end{pmatrix}$	$\begin{pmatrix} -t_{xx} - t_{xy} & 0 \\ t_{xy} & -t_{xx} & 0 \\ 0 & 0 & -t_{zz} \end{pmatrix}$	$\bar{3}1m'$	$\begin{pmatrix} \sigma_{xx} & \sigma_{xy} & 0 \\ -\sigma_{xy} & \sigma_{xx} & 0 \\ 0 & 0 & \sigma_{zz} \end{pmatrix}$	$\begin{pmatrix} \sigma_{xx}^z & \sigma_{xy}^z & 0 \\ -\sigma_{xy}^z & \sigma_{xx}^z & 0 \\ 0 & 0 & \sigma_{zz}^z \end{pmatrix}$
$31m'$	$\begin{pmatrix} t_{xx} & t_{xy} & 0 \\ -t_{xy} & t_{xx} & 0 \\ 0 & 0 & t_{zz} \end{pmatrix}$	$\begin{pmatrix} t_{xx} & t_{xy} & 0 \\ -t_{xy} & t_{xx} & 0 \\ 0 & 0 & t_{zz} \end{pmatrix}$	$\bar{3}1m'$	$\begin{pmatrix} \sigma_{xx} & \sigma_{xy} & 0 \\ -\sigma_{xy} & \sigma_{xx} & 0 \\ 0 & 0 & \sigma_{zz} \end{pmatrix}$	$\begin{pmatrix} \sigma_{xx}^z & \sigma_{xy}^z & 0 \\ -\sigma_{xy}^z & \sigma_{xx}^z & 0 \\ 0 & 0 & \sigma_{zz}^z \end{pmatrix}$
$\bar{3}'1m'$	$\begin{pmatrix} t_{xx} & 0 & 0 \\ 0 & t_{xx} & 0 \\ 0 & 0 & t_{zz} \end{pmatrix}$	$\begin{pmatrix} t_{xx} & 0 & 0 \\ 0 & t_{xx} & 0 \\ 0 & 0 & t_{zz} \end{pmatrix}$	$\bar{3}1m1'$	$\begin{pmatrix} \sigma_{xx} & 0 & 0 \\ 0 & \sigma_{xx} & 0 \\ 0 & 0 & \sigma_{zz} \end{pmatrix}$	$\begin{pmatrix} 0 & \sigma_{xy}^z & 0 \\ -\sigma_{xy}^z & 0 & 0 \\ 0 & 0 & 0 \end{pmatrix}$
$\bar{3}'1m$	$\begin{pmatrix} 0 & t_{xy} & 0 \\ -t_{xy} & 0 & 0 \\ 0 & 0 & 0 \end{pmatrix}$	$\begin{pmatrix} 0 & -t_{xy} & 0 \\ t_{xy} & 0 & 0 \\ 0 & 0 & 0 \end{pmatrix}$	$\bar{3}1m1'$	$\begin{pmatrix} \sigma_{xx} & 0 & 0 \\ 0 & \sigma_{xx} & 0 \\ 0 & 0 & \sigma_{zz} \end{pmatrix}$	$\begin{pmatrix} 0 & \sigma_{xy}^z & 0 \\ -\sigma_{xy}^z & 0 & 0 \\ 0 & 0 & 0 \end{pmatrix}$

Table IV. Table II continued for trigonal groups with  $O(k) = 3$ .

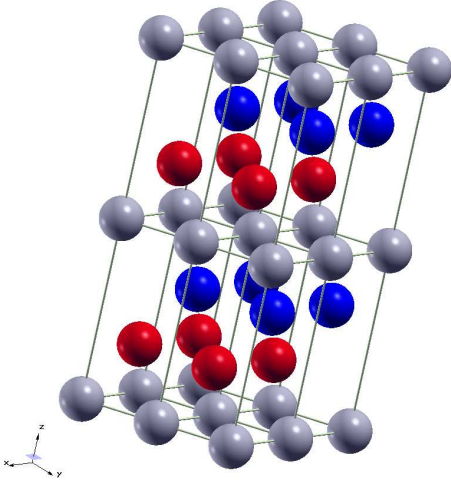


Figure 1. (Color online) Structure of the investigated multilayer system Pt|Fe<sub>x</sub>Co<sub>1-x</sub>|Cu consisting of a stacking of fcc (111) planes along the z axis. Cu atoms are colored in blue, Fe<sub>x</sub>Co<sub>1-x</sub> sites in red and Pt atoms are represented in light grey.

surface as well as Fermi sea terms (see Eq. (1)) when the Kubo-Bastin formula is used (see comment below). Corresponding results for Pt|Fe<sub>x</sub>Co<sub>1-x</sub>|Cu are shown in the middle panel of Fig. 2. As one notes, the Fermi surface and sea contributions are comparable in magnitude but have opposite sign leading to a partial cancellation. Obviously, both contributions vary rather smoothly with concentration and show for the considered concentration range ( $0.1 \leq x \leq 0.9$ ) in contrast for example to the binary alloys Fe<sub>x</sub>Pd<sub>1-x</sub> and Ni<sub>x</sub>Pd<sub>1-x</sub><sup>58</sup> practically no divergent behavior in the dilute limit ( $x \rightarrow 0$  or  $x \rightarrow 1$ ). As discussed before<sup>58</sup> a divergent behavior of  $\sigma_{xy}$  can be ascribed to a strong skew scattering contribution that

scales with the longitudinal conductivity  $\sigma_{xx}$ .<sup>63</sup> On the other hand, this extrinsic source for the transverse transport is accounted for by the contribution to  $\sigma_{xy}$  that is connected with the vertex corrections.<sup>58</sup> Inspecting Fig. 2 (middle) that shows results for the Fermi surface contribution to  $\sigma_{xy}$  obtained with and without the vertex corrections, one finds that these give rise only to minor corrections throughout the considered concentration regime. With the skew scattering mechanism being negligible and the intrinsic contribution dominating the system is obviously in the so-called dirty regime.<sup>63,64</sup> Considering the Fermi sea contribution to  $\sigma_{xy}$  (Fig. 2 middle) one finds no impact of the vertex corrections at all. This is in full line with the findings of Turek *et al.*<sup>65</sup> who could show (at least within the TB-LMTO-CPA formalism) that this property has to be fulfilled for formal reasons. As a consequence, this implies that the skew scattering mechanism is, as to be expected, connected only to the Fermi surface contribution to  $\sigma_{xy}$ . In fact, this is a seemingly trivial precondition to get the full skew scattering contribution to  $\sigma_{xy}$  when performing Boltzmann type of calculations for the dilute regime that are restricted to the Fermi energy  $E_F$ .<sup>66</sup> In fact, this is to be expected because for the electrical conductivity tensor it is possible for the case  $T = 0$  K to go from the Kubo-Bastin to the Kubo-Středa equation that has only contributions from the Fermi surface,<sup>50,67</sup> i.e., the Fermi sea term can be eliminated exactly.

Considering the spin conductivity tensor the non-vanishing tensor elements  $\sigma_{ij}^k$  can again be found from symmetry considerations.<sup>61</sup> Restricting here to the z component of the spin polarization one has the non-vanishing elements  $\sigma_{xx}^z = \sigma_{yy}^z \neq \sigma_{zz}^z$  and  $\sigma_{xy}^z = -\sigma_{yx}^z$ , i.e.,  $\underline{\sigma}^z$  has the same shape as  $\underline{\sigma}$ . Comparing the corresponding numerical results for the transverse spin conductivity shown in the lower panel of Fig. 2 with their counterparts connected with the transverse conductivity  $\sigma_{xy}$  one finds that a very similar behavior in the investigated concentration regime: i) the Fermi sea and

magnetic point group	$\underline{t}$	$\underline{t}'$	magnetic Laue group	$\underline{\sigma}$	$\underline{\sigma}^k$
$6'$	$\begin{pmatrix} t_{xx} & t_{xy} & 0 \\ -t_{xy} & t_{xx} & 0 \\ 0 & 0 & t_{zz} \end{pmatrix}$	$\begin{pmatrix} -t_{xx} & t_{xy} & 0 \\ -t_{xy} & -t_{xx} & 0 \\ 0 & 0 & -t_{zz} \end{pmatrix}$	$6'/m'$	$\begin{pmatrix} \sigma_{xx} & 0 & 0 \\ 0 & \sigma_{xx} & 0 \\ 0 & 0 & \sigma_{zz} \end{pmatrix}$	$\begin{pmatrix} \sigma_{xx}^z & \sigma_{xy}^z & 0 \\ -\sigma_{xy}^z & \sigma_{xx}^z & 0 \\ 0 & 0 & \sigma_{zz}^z \end{pmatrix}$
$\bar{6}'$	$\begin{pmatrix} t_{xx} & t_{xy} & 0 \\ -t_{xy} & t_{xx} & 0 \\ 0 & 0 & t_{zz} \end{pmatrix}$	$\begin{pmatrix} t_{xx} & -t_{xy} & 0 \\ t_{xy} & t_{xx} & 0 \\ 0 & 0 & t_{zz} \end{pmatrix}$	$6'/m'$	$\begin{pmatrix} \sigma_{xx} & 0 & 0 \\ 0 & \sigma_{xx} & 0 \\ 0 & 0 & \sigma_{zz} \end{pmatrix}$	$\begin{pmatrix} \sigma_{xx}^z & \sigma_{xy}^z & 0 \\ -\sigma_{xy}^z & \sigma_{xx}^z & 0 \\ 0 & 0 & \sigma_{zz}^z \end{pmatrix}$
$6/m'$	$\begin{pmatrix} t_{xx} & t_{xy} & 0 \\ -t_{xy} & t_{xx} & 0 \\ 0 & 0 & t_{zz} \end{pmatrix}$	$\begin{pmatrix} t_{xx} & -t_{xy} & 0 \\ t_{xy} & t_{xx} & 0 \\ 0 & 0 & t_{zz} \end{pmatrix}$	$6/m1'$	$\begin{pmatrix} \sigma_{xx} & 0 & 0 \\ 0 & \sigma_{xx} & 0 \\ 0 & 0 & \sigma_{zz} \end{pmatrix}$	$\begin{pmatrix} \sigma_{xx}^z & \sigma_{xy}^z & 0 \\ -\sigma_{xy}^z & \sigma_{xx}^z & 0 \\ 0 & 0 & \sigma_{zz}^z \end{pmatrix}$
$6'22'$	$\begin{pmatrix} t_{xx} & 0 & 0 \\ 0 & t_{xx} & 0 \\ 0 & 0 & t_{zz} \end{pmatrix}$	$\begin{pmatrix} -t_{xx} & 0 & 0 \\ 0 & -t_{xx} & 0 \\ 0 & 0 & -t_{zz} \end{pmatrix}$	$6'/m'mm'$	$\begin{pmatrix} \sigma_{xx} & 0 & 0 \\ 0 & \sigma_{xx} & 0 \\ 0 & 0 & \sigma_{zz} \end{pmatrix}$	$\begin{pmatrix} 0 & \sigma_{xy}^z & 0 \\ -\sigma_{xy}^z & 0 & 0 \\ 0 & 0 & 0 \end{pmatrix}$
$62'2'$	$\begin{pmatrix} t_{xx} & t_{xy} & 0 \\ -t_{xy} & t_{xx} & 0 \\ 0 & 0 & t_{zz} \end{pmatrix}$	$\begin{pmatrix} -t_{xx} & -t_{xy} & 0 \\ t_{xy} & -t_{xx} & 0 \\ 0 & 0 & -t_{zz} \end{pmatrix}$	$6/mm'm'$	$\begin{pmatrix} \sigma_{xx} & \sigma_{xy} & 0 \\ -\sigma_{xy} & \sigma_{xx} & 0 \\ 0 & 0 & \sigma_{zz} \end{pmatrix}$	$\begin{pmatrix} \sigma_{xx}^z & \sigma_{xy}^z & 0 \\ -\sigma_{xy}^z & \sigma_{xx}^z & 0 \\ 0 & 0 & \sigma_{zz}^z \end{pmatrix}$
$6'mm'$	$\begin{pmatrix} 0 & t_{xy} & 0 \\ -t_{xy} & 0 & 0 \\ 0 & 0 & 0 \end{pmatrix}$	$\begin{pmatrix} 0 & t_{xy} & 0 \\ -t_{xy} & 0 & 0 \\ 0 & 0 & 0 \end{pmatrix}$	$6'/m'mm'$	$\begin{pmatrix} \sigma_{xx} & 0 & 0 \\ 0 & \sigma_{xx} & 0 \\ 0 & 0 & \sigma_{zz} \end{pmatrix}$	$\begin{pmatrix} 0 & \sigma_{xy}^z & 0 \\ -\sigma_{xy}^z & 0 & 0 \\ 0 & 0 & 0 \end{pmatrix}$
$6m'm'$	$\begin{pmatrix} t_{xx} & t_{xy} & 0 \\ -t_{xy} & t_{xx} & 0 \\ 0 & 0 & t_{zz} \end{pmatrix}$	$\begin{pmatrix} t_{xx} & t_{xy} & 0 \\ -t_{xy} & t_{xx} & 0 \\ 0 & 0 & t_{zz} \end{pmatrix}$	$6/mm'm'$	$\begin{pmatrix} \sigma_{xx} & \sigma_{xy} & 0 \\ -\sigma_{xy} & \sigma_{xx} & 0 \\ 0 & 0 & \sigma_{zz} \end{pmatrix}$	$\begin{pmatrix} \sigma_{xx}^z & \sigma_{xy}^z & 0 \\ -\sigma_{xy}^z & \sigma_{xx}^z & 0 \\ 0 & 0 & \sigma_{zz}^z \end{pmatrix}$
$\bar{6}'2m'$	$\begin{pmatrix} t_{xx} & 0 & 0 \\ 0 & t_{xx} & 0 \\ 0 & 0 & t_{zz} \end{pmatrix}$	$\begin{pmatrix} t_{xx} & 0 & 0 \\ 0 & t_{xx} & 0 \\ 0 & 0 & t_{zz} \end{pmatrix}$	$6'/m'mm'$	$\begin{pmatrix} \sigma_{xx} & 0 & 0 \\ 0 & \sigma_{xx} & 0 \\ 0 & 0 & \sigma_{zz} \end{pmatrix}$	$\begin{pmatrix} 0 & \sigma_{xy}^z & 0 \\ -\sigma_{xy}^z & 0 & 0 \\ 0 & 0 & 0 \end{pmatrix}$
$\bar{6}'m2'$	$\begin{pmatrix} 0 & t_{xy} & 0 \\ -t_{xy} & 0 & 0 \\ 0 & 0 & 0 \end{pmatrix}$	$\begin{pmatrix} 0 & -t_{xy} & 0 \\ t_{xy} & 0 & 0 \\ 0 & 0 & 0 \end{pmatrix}$	$6'/m'mm'$	$\begin{pmatrix} \sigma_{xx} & 0 & 0 \\ 0 & \sigma_{xx} & 0 \\ 0 & 0 & \sigma_{zz} \end{pmatrix}$	$\begin{pmatrix} 0 & \sigma_{xy}^z & 0 \\ -\sigma_{xy}^z & 0 & 0 \\ 0 & 0 & 0 \end{pmatrix}$
$6/m'm'm'$	$\begin{pmatrix} t_{xx} & 0 & 0 \\ 0 & t_{xx} & 0 \\ 0 & 0 & t_{zz} \end{pmatrix}$	$\begin{pmatrix} t_{xx} & 0 & 0 \\ 0 & t_{xx} & 0 \\ 0 & 0 & t_{zz} \end{pmatrix}$	$6/mmm1'$	$\begin{pmatrix} \sigma_{xx} & 0 & 0 \\ 0 & \sigma_{xx} & 0 \\ 0 & 0 & \sigma_{zz} \end{pmatrix}$	$\begin{pmatrix} 0 & \sigma_{xy}^z & 0 \\ -\sigma_{xy}^z & 0 & 0 \\ 0 & 0 & 0 \end{pmatrix}$
$6/m'mm$	$\begin{pmatrix} 0 & t_{xy} & 0 \\ -t_{xy} & 0 & 0 \\ 0 & 0 & 0 \end{pmatrix}$	$\begin{pmatrix} 0 & -t_{xy} & 0 \\ t_{xy} & 0 & 0 \\ 0 & 0 & 0 \end{pmatrix}$	$6/mmm1'$	$\begin{pmatrix} \sigma_{xx} & 0 & 0 \\ 0 & \sigma_{xx} & 0 \\ 0 & 0 & \sigma_{zz} \end{pmatrix}$	$\begin{pmatrix} 0 & \sigma_{xy}^z & 0 \\ -\sigma_{xy}^z & 0 & 0 \\ 0 & 0 & 0 \end{pmatrix}$

Table V. Table II continued for hexagonal groups with  $O(k) = 6$ .

magnetic point group	$\underline{t}$	$\underline{t}'$	magnetic Laue group	$\underline{\sigma}$	$\underline{\sigma}^k$
$m'\bar{3}'$	$\begin{pmatrix} t_{xx} & 0 & 0 \\ 0 & t_{xx} & 0 \\ 0 & 0 & t_{xx} \end{pmatrix}$	$\begin{pmatrix} t_{xx} & 0 & 0 \\ 0 & t_{xx} & 0 \\ 0 & 0 & t_{xx} \end{pmatrix}$	$m\bar{3}1'$	$\begin{pmatrix} \sigma_{xx} & 0 & 0 \\ 0 & \sigma_{xx} & 0 \\ 0 & 0 & \sigma_{xx} \end{pmatrix}$	$\begin{pmatrix} 0 & \sigma_{xy}^z & 0 \\ \sigma_{xz}^z & 0 & 0 \\ 0 & 0 & 0 \end{pmatrix}$
$4'32'$	$\begin{pmatrix} t_{xx} & 0 & 0 \\ 0 & t_{xx} & 0 \\ 0 & 0 & t_{xx} \end{pmatrix}$	$\begin{pmatrix} -t_{xx} & 0 & 0 \\ 0 & -t_{xx} & 0 \\ 0 & 0 & -t_{xx} \end{pmatrix}$	$m\bar{3}m'$	$\begin{pmatrix} \sigma_{xx} & 0 & 0 \\ 0 & \sigma_{xx} & 0 \\ 0 & 0 & \sigma_{xx} \end{pmatrix}$	$\begin{pmatrix} 0 & \sigma_{xy}^z & 0 \\ \sigma_{xz}^z & 0 & 0 \\ 0 & 0 & 0 \end{pmatrix}$
$\bar{4}'3m'$	$\begin{pmatrix} t_{xx} & 0 & 0 \\ 0 & t_{xx} & 0 \\ 0 & 0 & t_{xx} \end{pmatrix}$	$\begin{pmatrix} t_{xx} & 0 & 0 \\ 0 & t_{xx} & 0 \\ 0 & 0 & t_{xx} \end{pmatrix}$	$m\bar{3}m'$	$\begin{pmatrix} \sigma_{xx} & 0 & 0 \\ 0 & \sigma_{xx} & 0 \\ 0 & 0 & \sigma_{xx} \end{pmatrix}$	$\begin{pmatrix} 0 & \sigma_{xy}^z & 0 \\ \sigma_{xz}^z & 0 & 0 \\ 0 & 0 & 0 \end{pmatrix}$
$m'\bar{3}'m'$	$\begin{pmatrix} t_{xx} & 0 & 0 \\ 0 & t_{xx} & 0 \\ 0 & 0 & t_{xx} \end{pmatrix}$	$\begin{pmatrix} t_{xx} & 0 & 0 \\ 0 & t_{xx} & 0 \\ 0 & 0 & t_{xx} \end{pmatrix}$	$m\bar{3}m1'$	$\begin{pmatrix} \sigma_{xx} & 0 & 0 \\ 0 & \sigma_{xx} & 0 \\ 0 & 0 & \sigma_{xx} \end{pmatrix}$	$\begin{pmatrix} 0 & \sigma_{xy}^z & 0 \\ -\sigma_{xy}^z & 0 & 0 \\ 0 & 0 & 0 \end{pmatrix}$

Table VI. Table II continued for cubic groups.

surface contributions are comparable in magnitude but have different sign leading to a pronounced cancellation, ii) the individual terms vary very weakly with concentration without showing any divergent behavior, iii) the Fermi surface contribution shows a very weak impact of the vertex contributions while, iv) the Fermi sea contribution is not affected at all by the vertex corrections. The

findings iii) and iv) again imply that the extrinsic contributions and with this the skew scattering contribution are very small. Finding iv) that so far has been demonstrated only numerically is now (in contact to the case of the electrical conductivity) by no means trivial. While the use of a Kubo-Středa-like equation for  $\sigma_{xy}^z$  turned out to be very successful when applied to metallic alloys<sup>59</sup> it



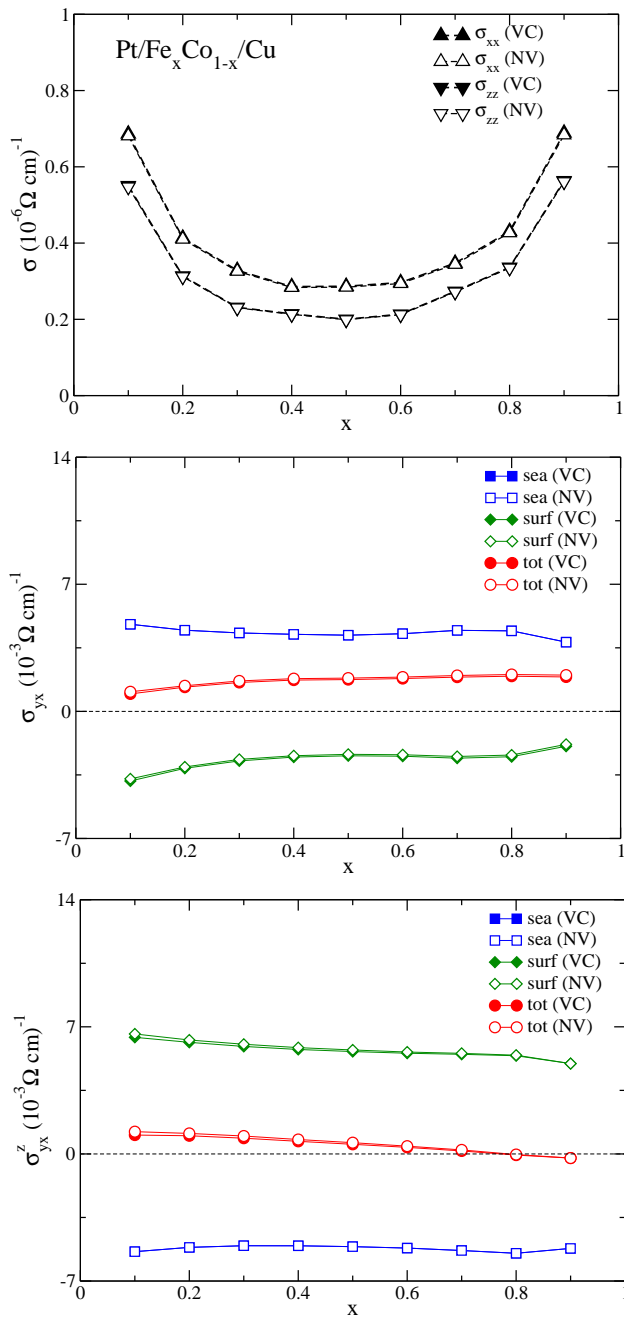


Figure 2. (Color online) Top: The longitudinal components  $\sigma_{xx} = \sigma_{yy}$  and  $\sigma_{zz}$  of the conductivity tensor  $\underline{\sigma}$  of Pt|Fe<sub>x</sub>Co<sub>1-x</sub>|Cu as a function of the concentration  $x$ . Middle: The corresponding anomalous Hall conductivity  $\sigma_{xy} = -\sigma_{yx}$ . Bottom: The spin Hall conductivity  $\sigma_{yx}^z = -\sigma_{xy}^z$ . Open symbols represent calculations without vertex corrections (NV) and filled symbols those including vertex corrections (VC). The blue squares correspond to the Fermi sea contribution (sea), the green diamonds represent contributions from the Fermi surface (surf) and red circles give the total result (tot).

has to be seen as approximate.<sup>68</sup> For that reason the finding that there are no vertex corrections to the Fermi sea part but only for the Fermi surface part is now an important precondition for getting all skew scattering contributions to  $\sigma_{xy}^z$  by performing calculations based on the Boltzmann equation.<sup>66,69,70</sup>

For the magnetization along the  $z$  axis Pt|Fe<sub>x</sub>Co<sub>1-x</sub>|Cu has the magnetic point group  $3m$ <sup>71</sup> leading to an anti-symmetric torque tensor with non-vanishing elements  $t_{xx} = t_{yy} \neq t_{zz}$  and  $t_{xy} = -t_{yx}$  (see row three of Tab. IV). Actually, because of the restrictions imposed by the form of the torque operator given in Eq. (2) the element  $t_{zz}$  that would represent a change in the magnitude of the magnetic moment along the  $z$  direction does not show up in the calculations. In fact, this impact of an external electric field can be considered as a manifestation of the Edelstein effect<sup>72,73</sup> and can be described by a response quantity formulated appropriately.<sup>74</sup> The top panel of Fig. 3 gives the numerical results for the diagonal torque element  $t_{xx}$ . As one can see, it has many properties in common with the longitudinal conductivity  $\sigma_{xx}$ : i) there is no Fermi sea contribution, ii) it shows a divergent behavior in the dilute limit  $x \rightarrow 0$  or  $x \rightarrow 1$ , respectively. In contrast to  $\sigma_{xx}$ , however, we find no impact of the vertex corrections at all. This implies that there are no contributions due to skew scattering and accordingly there is only an intrinsic contribution to  $t_{xx}$ . As a consequence, this torque tensor element will not be accessible by calculations based on the Boltzmann formalism. Considering  $t_{xy}$  one finds from Figs. 2 and 3 that this tensor element behaves much like  $\sigma_{xy}$  and  $\sigma_{xy}^z$ : i) the Fermi sea and surface contributions are comparable in magnitude but have different sign leading to a partial cancellation, ii) both parts are weakly concentration dependent with a more pronounced variation for the Fermi surface term on the Co-rich side, iii) the Fermi surface contribution shows a very weak impact of the vertex contributions, while iv) the Fermi sea contribution is not affected at all by the vertex contributions. Again, from iii) and iv) one may conclude that the extrinsic contributions due to the skew scattering are very small. In contrast to  $t_{xx}$  calculations based on the Boltzmann formalism should be able to account for this contribution to  $t_{xy}$ . The comparable concentration dependence of the spin Hall conductivity  $\sigma_{xy}^z$  and the even torque  $t_{xy}$  seems to support previous suggestions that they are intimately connected.<sup>75</sup>

The first *ab-initio* investigations on the spin-orbit torque by Freimuth *et al.*<sup>42,43</sup> were dealing among others with Co/Pt(111) having the same symmetry as the system Pt|Fe<sub>x</sub>Co<sub>1-x</sub>|Cu considered here. As shown by these authors, the mirror planes perpendicular to the atomic layers implies the  $t_{xx}$  and  $t_{xy}$  to be odd and even, respectively, under reversal of the magnetization direction, i.e., one has  $t_{xx}(\mathbf{m}) = -t_{xx}(-\mathbf{m})$  and  $t_{xy}(\mathbf{m}) = t_{xy}(-\mathbf{m})$ . Our numerical results are fully in

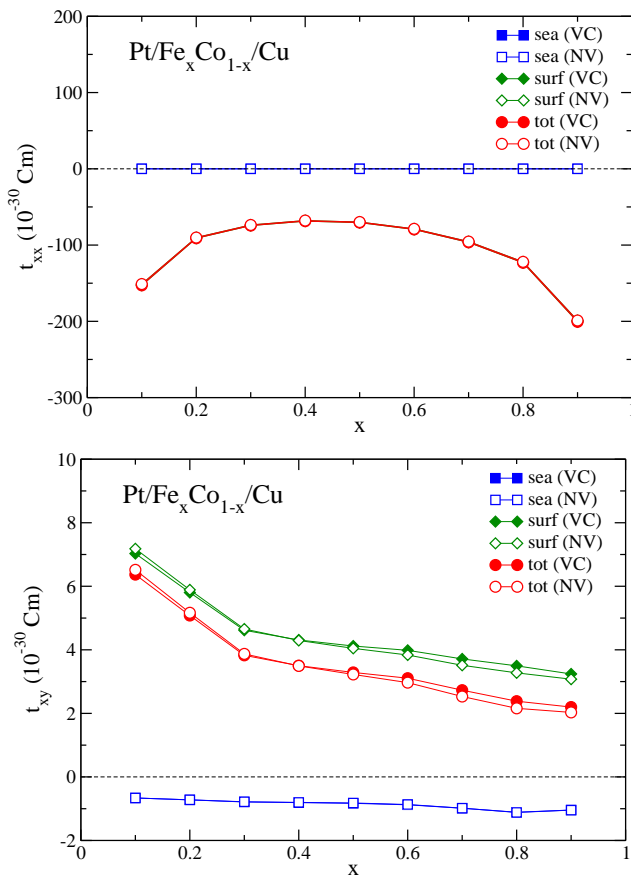


Figure 3. (Color online) Top: The longitudinal component  $t_{xx} = t_{yy}$  of the SOT depending on the concentration. Bottom: The transverse component  $t_{xy} = -t_{yx}$  of the SOT depending on the concentration. Use of symbols and colors as in Fig. 2.

line with this basic symmetry restriction. Freimuth *et al.* also used the Kubo-Bastin formalism, however, with the Green function represented in terms of Bloch functions and energy eigen values. This restricted the investigation to the very dilute limit with the impact of chemical or structural disorder represented by a broadening parameter  $\Gamma$ . Calculating the diagonal torkance element  $t_{xx}$  as a function of  $\Gamma$  leads in the limit  $\Gamma \rightarrow 0$  to a divergent behavior. This is obviously in full accordance with the results shown in Fig. 3 (top) that also show a divergence for the concentration  $x \rightarrow 0$  or  $x \rightarrow 1$ , implying that the major impact of disorder on the diagonal torkance is independent of whether it is accounted for within the framework of the CPA or the Gaussian disorder model.<sup>43</sup> The same applies also to the off-diagonal element  $t_{xy}$ . While  $t_{xy}$  given in Fig. 3 shows only a weak variation with concentration in the considered composition regime,  $t_{xy}$  of Co/Pt(111) as calculated by Freimuth *et al.*<sup>43</sup> as a function of the broadening parameter takes a constant

and finite value in the limit  $\Gamma \rightarrow 0$ , the intrinsic contribution to the torkance. Concerning the decomposition of the torkance into Fermi sea and Fermi surface contributions, the results in Fig. 3 are again in qualitative agreement with the findings of Freimuth *et al.*<sup>42,43</sup>: The odd torkance element  $t_{xx}$  (top) has no Fermi sea contribution whereas to the even  $t_{xy}$  (bottom) both, Fermi sea and Fermi surface, contribute significantly. Finally, as suggested before – amongst others by the aforementioned authors – the similar composition dependence of  $t_{xy}$  and the spin Hall conductivity  $\sigma_{xy}^z$  seems to support at least in part the notion “spin Hall”-torque.

#### IV. CONCLUSIONS

In summary, based on Kubo’s linear response formalism, the symmetry and magnitude of spin-orbit torques in metals and alloys can be investigated using group-theoretical considerations for the former and an implementation of the Kubo-Bastin formula for the torkance in a multiple-scattering framework for the latter. The resulting tensor shapes for direct and inverse torkance for all magnetic point groups allowing a finite magnetization have been presented. The former have been independently confirmed for a number of systems by numerical calculations. By investigating the concentration dependence of two symmetrically distinct tensor elements in an fcc (111) trilayer system, contact and extensions could be made to previous work concerning the various contributions to the SOT and possible underlying mechanisms. While the odd torkance was found to bear a striking resemblance to the electrical conductivity concerning its dependence on the alloy composition in the ferromagnetic layer, the even component could be demonstrated to behave more like the transverse transport properties anomalous and spin Hall conductivity. The key advantage of the CPA alloy theory over simpler models of disorder is the possibility to calculate material-specific parameters very efficiently, opening the way to a computational materials design approach to direct and inverse spin-orbit torques. As has been shown, the electronic contribution to the corresponding thermally-induced phenomena, direct and inverse thermal spin-orbit torques, can in principle be calculated from the torkance employing a Mott-like expression. Future work will focus on the close connection between direct and inverse SOT to direct and inverse Edelstein effect.

#### ACKNOWLEDGMENTS

The authors would like to thank the *Deutsche Forschungsgemeinschaft* (German Science Foundation, DFG) for financial support via the programmes SPP 1538 and SFB 689.

- \* [sebastian.wimmer@cup.uni-muenchen.de](mailto:sebastian.wimmer@cup.uni-muenchen.de)  
† [hubert.ebert@cup.uni-muenchen.de](mailto:hubert.ebert@cup.uni-muenchen.de)
- <sup>1</sup> A. Manchon and S. Zhang, *Phys. Rev. B* **78**, 212405 (2008).
  - <sup>2</sup> A. Manchon and S. Zhang, *Phys. Rev. B* **79**, 094422 (2009).
  - <sup>3</sup> I. Garate and A. H. MacDonald, *Phys. Rev. B* **80**, 134403 (2009).
  - <sup>4</sup> A. Chernyshov, M. Overby, X. Liu, J. K. Furdyna, Y. Lyanda-Geller, and L. P. Rokhinson, *Nat. Phys.* **5**, 656 (2009).
  - <sup>5</sup> I. Mihai Miron, G. Gaudin, S. Auffret, B. Rodmacq, A. Schuhl, S. Pizzini, J. Vogel, and P. Gambardella, *Nat. Mater.* **9**, 230 (2010).
  - <sup>6</sup> U. H. Pi, K. Won Kim, J. Y. Bae, S. C. Lee, Y. J. Cho, K. S. Kim, and S. Seo, *Applied Physics Letters* **97**, 162507 (2010).
  - <sup>7</sup> G. Gaudin, I. M. Miron, P. Gambardella, A. Schuhl, Magnetic memory element, Patent, US Patent application, 12/899,072, 12/899,091, 12/959,980, (2010).
  - <sup>8</sup> For alternatives to the SOT for *control of magnetism by electric fields* see for example the same-titled review by Matsukara *et al.*<sup>76</sup>.
  - <sup>9</sup> I. M. Miron, K. Garello, G. Gaudin, P.-J. Zermatten, M. V. Costache, S. Auffret, S. Bandiera, B. Rodmacq, A. Schuhl, and P. Gambardella, *Nature* **476**, 189 (2011).
  - <sup>10</sup> J. Slonczewski, *J. Magn. Magn. Materials* **159**, L1 (1996).
  - <sup>11</sup> L. Berger, *Phys. Rev. B* **54**, 9353 (1996).
  - <sup>12</sup> P. Gambardella and I. M. Miron, *Philosophical Transactions of the Royal Society of London A: Mathematical, Physical and Engineering Sciences* **369**, 3175 (2011).
  - <sup>13</sup> K. Garello, I. M. Miron, C. O. Avci, F. Freimuth, Y. Mokrousov, S. Blügel, S. Auffret, O. Boulle, G. Gaudin, and P. Gambardella, *Nat. Nanotechnol.* **8**, 587 (2013).
  - <sup>14</sup> J. Kim, J. Sinha, M. Hayashi, M. Yamanouchi, S. Fukami, T. Suzuki, S. Mitani, and H. Ohno, *Nat. Mater.* **12**, 240 (2013).
  - <sup>15</sup> X. Qiu, P. Deorani, K. Narayanapillai, K.-S. Lee, K.-J. Lee, H.-W. Lee, and H. Yang, *Scientific Reports* **4**, 4491 (2014).
  - <sup>16</sup> I. M. Miron, T. Moore, H. Szambolics, L. D. Buda-Prejbeanu, S. Auffret, B. Rodmacq, S. Pizzini, J. Vogel, M. Bonfim, A. Schuhl, and G. Gaudin, *Nat. Mater.* **10**, 419 (2011).
  - <sup>17</sup> L. Liu, O. J. Lee, T. J. Gudmundsen, D. C. Ralph, and R. A. Buhrman, *Phys. Rev. Lett.* **109**, 096602 (2012).
  - <sup>18</sup> L. Liu, C.-F. Pai, Y. Li, H. W. Tseng, D. C. Ralph, and R. A. Buhrman, *Science* **336**, 555 (2012).
  - <sup>19</sup> H. Reichlová, D. Kriegner, V. Holý, K. Olejník, V. Novák, M. Yamada, K. Miura, S. Ogawa, H. Takahashi, T. Jungwirth, and J. Wunderlich, *Phys. Rev. B* **92**, 165424 (2015).
  - <sup>20</sup> V. Tshitoyan, C. Ciccarelli, A. P. Mihai, M. Ali, A. C. Irvine, T. A. Moore, T. Jungwirth, and A. J. Ferguson, *Phys. Rev. B* **92**, 214406 (2015).
  - <sup>21</sup> W. Zhang, M. B. Jungfleisch, F. Freimuth, W. Jiang, J. Sklenar, J. E. Pearson, J. B. Ketterson, Y. Mokrousov, and A. Hoffmann, *Phys. Rev. B* **92**, 144405 (2015).
  - <sup>22</sup> S. Fukami, C. Zhang, S. DuttaGupta, A. Kurenkov, and H. Ohno, *Nat. Mater.* **advance online publication** (2016).
  - <sup>23</sup> J. Železný, H. Gao, K. Výborný, J. Zemen, J. Mašek, A. Manchon, J. Wunderlich, J. Sinova, and T. Jungwirth, *Phys. Rev. Lett.* **113**, 157201 (2014).
  - <sup>24</sup> A. Hamadeh, O. d'Allivy Kelly, C. Hahn, H. Meley, R. Bernard, A. H. Molpeceres, V. V. Naletov, M. Viret, A. Anane, V. Cros, S. O. Demokritov, J. L. Prieto, M. Muñoz, G. de Loubens, and O. Klein, *Phys. Rev. Lett.* **113**, 197203 (2014).
  - <sup>25</sup> Y. Fan, P. Upadhyaya, X. Kou, M. Lang, S. Takei, Z. Wang, J. Tang, L. He, L.-T. Chang, M. Montazeri, G. Yu, W. Jiang, T. Nie, R. N. Schwartz, Y. Tserkovnyak, and K. L. Wang, *Nat. Mater.* **13**, 699 (2014).
  - <sup>26</sup> Y. Wang, P. Deorani, K. Banerjee, N. Koirala, M. Brahlek, S. Oh, and H. Yang, *Phys. Rev. Lett.* **114**, 257202 (2015).
  - <sup>27</sup> G. Yu, P. Upadhyaya, Y. Fan, J. G. Alzate, W. Jiang, K. L. Wong, S. Takei, S. A. Bender, L.-T. Chang, Y. Jiang, M. Lang, J. Tang, Y. Wang, Y. Tserkovnyak, P. K. Amiri, and K. L. Wang, *Nat. Nanotechnol.* **9**, 548 (2014).
  - <sup>28</sup> M. Cubukcu, O. Boulle, M. Drouard, K. Garello, C. Onur Avci, I. Mihai Miron, J. Langer, B. Ocker, P. Gambardella, and G. Gaudin, *Applied Physics Letters* **104**, 042406 (2014).
  - <sup>29</sup> G. Prenat, K. Jabeur, G. Pendina, O. Boulle, and G. Gaudin, “Spintronics-based computing,” (Springer International Publishing, Cham, 2015) Chap. Beyond STT-MRAM, Spin Orbit Torque RAM SOT-MRAM for High Speed and High Reliability Applications, pp. 145–157.
  - <sup>30</sup> C. K. Safeer, E. Jué, A. Lopez, L. Buda-Prejbeanu, S. Auffret, S. Pizzini, O. Boulle, I. M. Miron, and G. Gaudin, *Nat. Nanotechnol.* **11**, 143 (2016).
  - <sup>31</sup> M. Yang, K. Cai, H. Ju, K. W. Edmonds, G. Yang, S. Liu, B. Li, B. Zhang, Y. Sheng, S. Wang, Y. Ji, and K. Wang, *Scientific Reports* **6**, 20778 (2016).
  - <sup>32</sup> A. Matos-Abiague and R. L. Rodríguez-Suárez, *Phys. Rev. B* **80**, 094424 (2009).
  - <sup>33</sup> K.-W. Kim, J.-H. Moon, K.-J. Lee, and H.-W. Lee, *Phys. Rev. Lett.* **108**, 217202 (2012).
  - <sup>34</sup> G. Tatara, N. Nakabayashi, and K.-J. Lee, *Phys. Rev. B* **87**, 054403 (2013).
  - <sup>35</sup> L. Liu, T. Moriyama, D. C. Ralph, and R. A. Buhrman, *Phys. Rev. Lett.* **106**, 036601 (2011).
  - <sup>36</sup> I. Garate and A. MacDonald, *Phys. Rev. B* **79**, 064403 (2009).
  - <sup>37</sup> P. M. Haney, H.-W. Lee, K.-J. Lee, A. Manchon, and M. D. Stiles, *Phys. Rev. B* **87**, 174411 (2013).
  - <sup>38</sup> A. Manchon, [arXiv:1204.4869 \[cond-mat.mes-hall\]](https://arxiv.org/abs/1204.4869) (2012).
  - <sup>39</sup> H. Kurebayashi, J. Sinova, D. Fang, A. C. Irvine, T. D. Skinner, J. Wunderlich, V. Novak, R. P. Campion, B. L. Gallagher, E. K. Vehstedt, P. L. Zarbo, K. Vyborny, A. J. Ferguson, and T. Jungwirth, *Nat. Nanotechnol.* **9**, 211 (2014).
  - <sup>40</sup> K.-W. Kim, K.-J. Lee, H.-W. Lee, and M. D. Stiles, *Phys. Rev. B* **92**, 224426 (2015).
  - <sup>41</sup> P. M. Haney, H.-W. Lee, K.-J. Lee, A. Manchon, and M. D. Stiles, *Phys. Rev. B* **88**, 214417 (2013).
  - <sup>42</sup> F. Freimuth, S. Blügel, and Y. Mokrousov, *J. Phys.: Cond. Mat.* **26**, 104202 (2014).
  - <sup>43</sup> F. Freimuth, S. Blügel, and Y. Mokrousov, *Phys. Rev. B* **90**, 174423 (2014).
  - <sup>44</sup> K. M. D. Hals, A. Brataas, and Y. Tserkovnyak, *EPL (Europhysics Letters)* **90**, 47002 (2010).
  - <sup>45</sup> C. Ciccarelli, H. M. D., A. Irvine, V. Novak, Y. Tserkovnyak, H. Kurebayashi, A. Brataas, and A. Ferguson, *Nat. Nanotechnol.* **10**, 50 (2015).

- <sup>46</sup> F. Freimuth, S. Blügel, and Y. Mokrousov, *Phys. Rev. B* **92**, 064415 (2015).
- <sup>47</sup> G. Géranton, F. Freimuth, S. Blügel, and Y. Mokrousov, *Phys. Rev. B* **91**, 014417 (2015).
- <sup>48</sup> F. Freimuth, S. Blügel, and Y. Mokrousov, ArXiv e-prints (2016), [arXiv:1602.03319 \[cond-mat.mes-hall\]](https://arxiv.org/abs/1602.03319).
- <sup>49</sup> A. Bastin, C. Lewiner, O. Betbeder-matibet, and P. Nozières, *J. Phys. Chem. Solids* **32**, 1811 (1971).
- <sup>50</sup> A. Crépieux and P. Bruno, *Phys. Rev. B* **64**, 014416 (2001).
- <sup>51</sup> The expression for the torque tensor given here differs slightly from that given by Freimuth *et al.*<sup>42,43</sup> but is in full accordance with the corresponding expression for the conductivity tensor as given for example by Crépieux and Bruno<sup>50</sup>.
- <sup>52</sup> M. E. Rose, *Relativistic Electron Theory* (Wiley, New York, 1961).
- <sup>53</sup> H. Ebert, S. Mankovsky, D. Ködderitzsch, and P. J. Kelly, *Phys. Rev. Lett.* **107**, 066603 (2011).
- <sup>54</sup> A. H. MacDonald and S. H. Vosko, *J. Phys. C: Solid State Phys.* **12**, 2977 (1979).
- <sup>55</sup> H. Ebert, in *Electronic Structure and Physical Properties of Solids*, Lecture Notes in Physics, Vol. 535, edited by H. Dreyssé (Springer, Berlin, 2000) p. 191.
- <sup>56</sup> H. Ebert, D. Ködderitzsch, and J. Minár, *Rep. Prog. Phys.* **74**, 096501 (2011).
- <sup>57</sup> W. H. Butler, *Phys. Rev. B* **31**, 3260 (1985).
- <sup>58</sup> S. Lowitzer, D. Ködderitzsch, and H. Ebert, *Phys. Rev. Lett.* **105**, 266604 (2010).
- <sup>59</sup> S. Lowitzer, M. Gradhand, D. Ködderitzsch, D. V. Fedorov, I. Mertig, and H. Ebert, *Phys. Rev. Lett.* **106**, 056601 (2011).
- <sup>60</sup> W. H. Kleiner, *Phys. Rev.* **142**, 318 (1966).
- <sup>61</sup> M. Seemann, D. Ködderitzsch, S. Wimmer, and H. Ebert, *Phys. Rev. B* **92**, 155138 (2015).
- <sup>62</sup> J. Banhart, H. Ebert, and A. Vernes, *Phys. Rev. B* **56**, 10165 (1997).
- <sup>63</sup> N. Nagaosa, J. Sinova, S. Onoda, A. H. MacDonald, and N. P. Ong, *Rev. Mod. Phys.* **82**, 1539 (2010).
- <sup>64</sup> R. Bianco, R. Resta, and I. Souza, *Phys. Rev. B* **90**, 125153 (2014).
- <sup>65</sup> I. Turek, J. Kudrnovský, and V. Drchal, *Phys. Rev. B* **89**, 064405 (2014).
- <sup>66</sup> B. Zimmermann, K. Chadova, D. Ködderitzsch, S. Blügel, H. Ebert, D. V. Fedorov, N. H. Long, P. Mavropoulos, I. Mertig, Y. Mokrousov, and M. Gradhand, *Phys. Rev. B* **90**, 220403 (2014).
- <sup>67</sup> P. Středa, *J. Phys. C: Solid State Phys.* **15**, L717 (1982).
- <sup>68</sup> D. Ködderitzsch, K. Chadova, and H. Ebert, *Phys. Rev. B* **92**, 184415 (2015).
- <sup>69</sup> M. Gradhand, D. V. Fedorov, P. Zahn, and I. Mertig, *Phys. Rev. Lett.* **104**, 186403 (2010).
- <sup>70</sup> C. Herschbach, D. V. Fedorov, I. Mertig, M. Gradhand, K. Chadova, H. Ebert, and D. Ködderitzsch, *Phys. Rev. B* **88**, 205102 (2013).
- <sup>71</sup> More precisely  $31m'$  or  $3m'1$ , depending on the axis convention for the corresponding space group. Results for the former are given here, the tensors for the other can be obtained by a rotation of the coordinate system by  $\pi/2$  around the principal axis. See Ref. 61 for details.
- <sup>72</sup> A. G. Aronov and Y. B. Lyanda-Geller, *JETP Lett.* **50**, 431 (1989).
- <sup>73</sup> V. M. Edelstein, *Solid State Commun.* **73**, 233 (1990).
- <sup>74</sup> The close connection between spin-orbit torques and the Edelstein effect has already been mentioned earlier<sup>46,77,78</sup> and will be discussed in detail elsewhere<sup>79</sup>.
- <sup>75</sup> See, e.g., Eq. (76) of Ref. 46 for an explicit relation.
- <sup>76</sup> F. Matsukura, Y. Tokura, and H. Ohno, *Nat. Nanotechnol.* **10**, 209 (2015).
- <sup>77</sup> H. Li, H. Gao, L. P. Zârbo, K. Vyborný, X. Wang, I. Garate, F. Doğan, A. Čejchan, J. Sinova, T. Jungwirth, and A. Manchon, *Phys. Rev. B* **91**, 134402 (2015).
- <sup>78</sup> T. D. Skinner, K. Olejník, L. K. Cunningham, H. Kurebayashi, R. P. Campion, B. L. Gallagher, T. Jungwirth, and A. J. Ferguson, *Nat. Commun.* **6**, 6730 (2015).
- <sup>79</sup> S. Wimmer, K. Chadova, M. Seemann, D. Ködderitzsch, and H. Ebert (unpublished).